



Published in final edited form as:

*Mol Imaging Biol.* 2019 April ; 21(2): 200–218. doi:10.1007/s11307-018-1239-2.

## Fluorescence Guidance in Surgical Oncology: Challenges, Opportunities, and Translation

Madeline T. Olson<sup>1,2</sup>, Quan P. Ly<sup>2,3</sup>, Aaron M. Mohs<sup>\*,2,4,5</sup>

<sup>1</sup>Eppley Institute for Research in Cancer and Allied Diseases, University of Nebraska Medical Center, Omaha, NE 68198

<sup>2</sup>Fred and Pamela Buffet Cancer Center, University of Nebraska Medical Center, Omaha, NE 68198

<sup>3</sup>Departments of Surgery, University of Nebraska Medical Center, Omaha, NE 68198

<sup>4</sup>Pharmaceutical Sciences, University of Nebraska Medical Center, Omaha, NE 68198

<sup>5</sup>Biochemistry and Molecular Biology, University of Nebraska Medical Center, Omaha, NE 68198

### Abstract

Surgical resection continues to function as the primary treatment option for most solid tumors. However, the detection of cancerous tissue remains predominantly subjective and reliant on the expertise of the surgeon. Surgery that is guided by fluorescence imaging has shown clinical relevance as a new approach to detecting the primary tumor, tumor margins, and metastatic lymph nodes. It is a technique to reduce recurrence and increase the possibility of a curative resection. While significant progress has been made in developing this emerging technology as a tool to assist the surgeon, further improvements are still necessary. Refining imaging agents and tumor targeting strategies to be a precise and reliable surgical strategy is essential in order to translate this technology into patient care settings. This review seeks to provide a comprehensive update on the most recent progress of fluorescence guided surgery and its translation into the clinic. By highlighting the current status and recent developments of fluorescence image guided surgery in the field of surgical oncology, we aim to offer insight into the challenges and opportunities that require further investigation.

### Keywords

Image-guided surgery; optical surgical navigation; surgical oncology; fluorescence; optical contrast agents

---

\*Correspondence to: Aaron M. Mohs, Ph.D. Department of Pharmaceutical Sciences University of Nebraska Medical Center 5-12315 Scott Research Tower Fred and Pamela Buffett Cancer Center Omaha, NE 68198-6858 aaron.mohs@unmc.edu.

Conflict of Interest: AMM is a co-inventor of image-guided surgery technology that is licensed to SpectroPath, Inc. (Atlanta, GA)

## Optical Surgical Navigation

### Clinical Relevance

With over 14 million estimated new cases, and 8 million deaths reported in the most recent *World Cancer Report*, cancer remains a leading cause of death across the globe [1]. In the United States alone, over 1.73 million new cases of cancer and over 600,000 deaths are estimated in 2018 [2]. Despite significant expansion and diversification of treatment options, surgical resection continues to serve as the cornerstone of treatment for most solid cancers. However, there are many complexities to tumor resections that require further investigation and/or improvement. Complete tumor resection relies on a surgeon's ability to differentiate between malignant and benign tissue using palpable and visual cues, but the infiltrative nature of cancerous tissue can make it difficult for surgeons to remove the entire tumor. The lack of differentiation, involvement of critical nerves and vasculature, and the stage of disease progression can complicate a tumor resection and lead to either incomplete removal or removal with significant morbidity [3]. If the tumor is not removed in its entirety, the residual cells at the surgical margin that result in positive margins, can lead to disease recurrence [4–6].

Fluorescence image-guided surgery (FIGS) offers a strategy to assist surgeons in delineating cancerous tissue through the use of fluorescence. Using this technology to color code the surgical field would better equip surgeons with the visual information needed to remove the tumor in its entirety or abort if needed, avoid inadvertent injury to non-cancerous tissue, confirm cancerous lymph nodes and metastases, and decrease disease recurrence.

FIGS may not be an equally beneficial solution for all cancer types. For example, in both ovarian and pancreatic cancers, the disease is often highly advanced and metastatic upon detection [7, 8].

Only 20% of pancreatic cancer patients are candidates for resection because of the aggressive dissemination of the disease and the high degree of involvement of the surrounding vasculature [9–12]. Even pancreatic cancer patients who undergo surgical resection, 80% will eventually succumb to disease recurrence [8, 10]. In ovarian cancer, it is common that patients undergo debulking surgery to leave less than one centimeter of residual disease, but because of the advanced stage of the disease, adjuvant chemotherapy is often used in conjunction with resection in an attempt to ablate microscopic disease [7, 13]. However, like pancreatic cancer, most patients with ovarian cancer develop recurrent disease [14]. To make surgical resection a viable and curative treatment option for highly metastatic cancers such as these, the development of early detection biomarkers is essential.

In addition to highlighting the primary tumor, FIGS may play a critical role in detecting early peritoneal disease and preventing inadvertent damage to critical and healthy tissue. Fluorescent detection of early peritoneal disease can reduce the number of unnecessary subsequent surgeries required to remove undetected metastatic disease [15, 16]. Nerve damage is a potential complication during surgical resection, especially in prostate and head and neck cancers, among others, because the fine innervations are difficult to differentiate from the tumor tissue. Damage to nerves during surgical resection can result in increased

post-operative morbidity, including increased pain and impaired function [17, 18]. Extensive nerve identification during surgery often results in prolonged operation time and possible damage to surrounding tissue [19]. However, the use of FIGS has shown efficacy in labeling the nerves to avoid this type of injury during resection [17, 20–22].

### Contrast Agents

Contrast agents applicable to FIGS generally fall into two categories; either visible or near infrared (NIR) dyes. NIR dyes (~700–1000 nm) offer potential advantages compared to visible dyes because of increased depth of light penetration, decreased light scattering, and lower tissue autofluorescence in the NIR region [23]. The properties of NIR fluorophores provide the high signal to noise ratio (SNR) required to aid surgeons in better differentiating cancerous tissue from normal tissue. Table 1 summarizes the properties of contrast agents that are frequently investigated for FIGS, including methylene blue, 5-aminolevulinic acid (5-ALA), cyanine-based dyes, including indocyanine green (ICG), IRDye800, and Dyomics dyes, and quantum dots. Fluorescein was an early dye used to illuminate tumors, but it is no longer as prevalent for FIGS because of its high autofluorescence and low tissue penetration [24]. Additionally, several cases have reported fluorescein causing anaphylactic shock [25, 26]. Each contrast currently used for FIGS comes with its own considerations, emission wavelength, quantum yield, toxicity, accumulation, and regulatory approval.

### Methylene Blue

Methylene blue is a widely utilized, FDA approved, visible wavelength dye [27]. This dye was developed as an alternative to its predecessor, isosulfan blue (Lymphazurin). Because there was a shortage of isosulfan blue when sentinel lymph node mapping was accepted as the staging modality for breast cancer and melanoma, methylene blue is now commonly used instead. Furthermore, there were reports of a 1–3% incidence rate of anaphylaxis with isosulfan blue. There have been reports of anaphylactic shock with methylene blue, but the rate is much lower. Regardless, the use of this dye is limited during pregnancy, because of its teratogenic potential [28, 29]. Nevertheless, this contrast agent has many applications for FIGS, as well as photodynamic therapy for cancer [30]. Previous studies have demonstrated the efficacy of this dye in identifying vital structures such as parathyroid glands, nerves, and ureters, to avoid injury during cancer resection [31–35]. Additionally, methylene blue has been used to identify sentinel lymph nodes and the presence of certain tumors [36–40]. However, uptake of this dye is highly variable and dependent on tumor type. Methylene blue is further limited because it lacks the favorable properties of NIR dyes, and it requires a high dose for detection in order to overcome autofluorescence [27].

### 5-ALA

5-ALA is a visible wavelength dye that was recently FDA approved for use as a fluorescent imaging agent in patients with high grade gliomas. A precursor molecule of the hemoglobin synthesis pathway, 5-ALA catalyzes the production and accumulation of the compound protoporphyrin IX (PpIX) in cancerous tissue. This compound exhibits fluorescence when excited by a violet-blue light source (405 nm), allowing for the visualization of cancerous tissue [41, 42]. The use of 5-ALA is associated with high specificity and positive predictive values [43]. However, while improved resection with 5-ALA correlates to improved survival

rates, there are also limitations to the use of this contrast agent, particularly its inconsistency [44]. Visible fluorescence is uncommon in low grade gliomas, and thus the usage of 5-ALA guided resection is restricted to solely higher grades. Previous studies have noted variance in the type of fluorescence, including both solid red fluorescence in the tumor tissue, and vague pink fluorescence at the transition zone between normal and cancerous tissue [45]. In areas of lower fluorescence, the ability of the dye to accurately identify cancerous tissue is sacrificed, thus poor sensitivity and low negative prediction values remain concerns for the use of 5-ALA [27, 41, 43, 44, 46].

## ICG

ICG is an FDA-approved NIR tricyanocyanine dye that has many uses in the clinic, and expanding uses in FIGS. This dye has very low toxicity, and has been approved for use in determining hepatic function, cardiac output, and ophthalmic perfusion for decades [27, 47]. ICG has also shown efficacy for FIGS in sentinel lymph node mapping, evaluating blood flow in reconstructed organs, and identifying and marking tumors for a variety of different solid cancer types [47–52]. Because ICG is a NIR dye, it is able to more deeply penetrate tissues, making it a good candidate for real-time FIGS. This dye is widely used across clinical trials and patient care settings, and has shown great potential for use with FIGS. However, ICG is limited by its aqueous instability, short circulation time, and concentration-dependent quenching. ICG also lacks the functional groups necessary for conjugation, rendering it a non-specific contrast agent. However, studies have shown that encapsulation of ICG improves its targeting abilities and circulation time, offering solutions to improve ICG for FIGS use. [53, 54].

## Dyes on the Rise

While 5-ALA, Methylene Blue, and ICG are the most prominent dyes entering clinics and clinical trials, many other contrast agents are showing significant promise in the pre-clinical phases. Cyanine derivatives (e.g. Cy7.5) and those developed by Dyomics (Jena, Germany) and LI-COR (Lincoln, NE, USA) Dy800, quantum dots, and others have been adapted for FIGS use in preclinical investigations (Table 1). IRDye800 (LI-COR) is perhaps the most advanced, appearing in current clinical trials, particularly in conjugation with antibodies [55–57]. The use of cyanine dyes overall, however, is still mostly restricted to the laboratory, but the conjugatable nature, stability, and high fluorescent capabilities of these dyes suggest potential for further success and clinical translation in the future [58, 59]. Quantum dots have also demonstrated significant potential for use in bioimaging applications, but concerns with safety and toxicity, especially the release of heavy metal ions and generation of reactive oxygen species, need to be addressed [60]. Development of non-toxic and biocompatible quantum dots is the next step towards clinical translation [61].

## Instrumentation

FIGS is advantageous to other imaging modalities such as x-ray computed tomography (CT) or magnetic resonance imaging (MRI) because it is less expensive, more mobile, and more feasible for integration into the surgical theatre [66]. Additionally, FIGS provides surgeons with real-time intraoperative feedback. FIGS also lacks the ionizing-radiation used in other imaging modalities, and is seen as extremely safe for use with clinically approved contrast

agents and probes [30]. A typical FIGS instrument has three main optical components: an excitation source, a collection source, and a display (Fig. 1). The excitation source must be able to excite the fluorophore at a working distance from the surgical field and emit a light that does not overlap with the emission wavelength of the fluorophore. Ideally, excitation light should be centered around the peak absorption wavelength for the fluorophore in use [67]. Common excitation sources are laser diodes, light-emitting diodes (LED), or filtered broadband lamps. Filtered broadband lamps are not ideal for image guided surgery because they are inefficient. These lamps produce excessive heat and lose significant optical power on the surgical field. Additionally, many photons must be discarded in order to produce a narrow enough band of excitation [68–70]. Therefore, LEDs and laser diodes are preferential for use in FIGS. However, each of these comes with its own considerations as well. LEDs provide a compromise of adequate efficiency, spectral confinement, and cost. However, heat dissipation is also a concern for this type of excitation source [67]. Laser diodes are the most precise in terms of spatial and spectral confinement, but raise concerns in terms of safety and cost [66, 68]. The collection source plays a critical role in FIGS instrumentation in transmitting the NIR signal from the excited fluorophore to the camera for interpretation. The sensitivity of detection is greatly determined by the background signal. In order to achieve a high level of sensitivity for the NIR signal, the FIGS hardware must be able to filter out and minimize background light. Differences in hardware design and emission filtration techniques can play a critical role in limiting the background signal and improving the sensitivity of FIGS instrumentation. [68–70]. Display monitors are the most common form of image display that are used to integrate the NIR and surgical field images to provide real-time feedback to surgeons. Most current display monitors feature an image of the surgical field next to an image of the NIR region on the surgical field. Previous designs have suggested developing a more seamless integration by superimposing the NIR image onto the image of the surgical field [3]. A recent review by Dsouza, et al. extensively compares current FIGS instrumentation systems and their efficacy, as well as features of FIGS systems that are most valued for clinical implementation. Increasing sensitivity to low contrast agent concentrations, obtaining quantification of fluorophore concentration, and adapting to multi-fluorophore imaging capabilities, are important considerations for FIGS instrumentation development [69].

## **Tumor Targeting Strategies – Passive**

### **Selective Accumulation**

The strategy of passive targeting was derived from the observation that certain macromolecules preferentially accumulate in tumors [71–73]. Passive targeting for the delivery of both free and conjugated contrast agents for FIGS exploits the enhanced permeability and retention (EPR) effect to provide selective and preferential accumulation of contrast agents in tumor tissue, as shown in Fig. 2. The biological basis for this phenomenon stems from the unique properties of vasculature and lymphatics in the tumor microenvironment. As tumors increase in size, inadequate delivery of oxygen and vital nutrients create a hypoxic environment in the center of the tumor. This hypoxic condition induces the expression of angiogenic growth factors to form neovasculature that will support the rapidly proliferating cells [74]. However, the architecture of this new vasculature is

irregularly dilated, highly disorganized, and hyper-permeable [75–77]. A loosened association between pericytes and endothelial cells further contributes to the vascular abnormality and hyper-permeability [78]. In addition to faulty vasculature, poor lymphatic distribution and the markedly impaired lymphatic drainage in the tumor [79, 80] create a retentive tumor environment that can potentially be utilized in FIGS due to the deposition of contrast agents in the tumor tissue [81, 82].

### Challenges to Implementation

Despite its proposed efficacy, there are many challenges involved with the implementation of EPR as a potential mechanism for contrast agent delivery. One criticism of this method of delivery is its relatively modest results, suggesting less than a 2-fold increase in delivery to tumor tissues in comparison to normal tissues [83, 84]. Because of the heterogeneity of tumors, it is difficult to predict the extent of the EPR in a specific patient. Tumor size, location, and organ type all play a role in the magnitude and presence of the EPR effect. While the unique characteristics of the tumor microenvironment are credited for the generation of the EPR effect, the same biological factors can significantly impede the efficacy of the phenomenon. For example, as depicted in Fig. 2b–e, heterogeneous perfusion, gradients of tumor cell growth, stress from the tumor stroma (including fibroblasts, mesenchymal cells, and immune cells), and high interstitial fluid pressure can contribute to the impediment of contrast agent delivery [83–85]. Tumor vasculature abnormalities often result in areas of poor and heterogeneous perfusion throughout the tumor. While the leaky tumor vasculature may contribute to contrast agent retention, heterogeneous blood flow can impede the homogenous delivery of contrast agents in the tumor tissue [85]. These variations in blood supply also lead to obscure gradients in tumor cell growth. While tumor cells proliferate rapidly near the vasculature, proliferation decreases at sites distant to the vasculature. The high density of proliferating cells surrounding the vasculature can compress blood vessels and lymphatics, preventing the convection of contrast agents in certain regions of the tumor [86–88]. Increasing density of tumor cell growth combined with poor lymphatic drainage result in very high interstitial pressure inside of the tumor. While the dense tumor center has a very high interstitial fluid pressure, there is a significant drop in pressure at the tumor periphery, which may result in the leakage of contrast agents into the peritumoral tissue [85, 89, 90]. The dense extracellular matrix of the tumor stroma further amplifies the solid stress in the tumor, constructing a collagen-rich network that hinders uniform contrast agent deposition [84, 85, 91]. Given the extent of the biological barriers, the EPR must be validated and improved upon. Otherwise, insufficient and unpredictable contrast agent delivery may render passive targeting an obsolete strategy for FIGS.

### Proposed Strategies for Improved Implementation

While there is significant controversy surrounding the prevalence and usefulness of the EPR effect, current research has demonstrated potential strategies to reorganize the tumor microenvironment to improve the EPR as well as use the presence of the EPR as a biomarker. Microenvironment alteration strategies include modifying tumor vasculature and blood flow, increasing vascular permeability, modulating the tumor stroma, and killing cancer cells [83, 84, 92–94]. Isolating biomarkers for the presence of the EPR effect has also

been suggested to identify potential candidates for receiving nanotherapeutics and passive delivery of contrast agents [95–97]. The implications of the EPR in personalized medicine, as well as the regulatory appeal, recognize the potential and translational importance of the EPR effect. Compared to highly specific targeted probes, passive targeting via the EPR effect is advantageous in its use of generic fluorescent probes, such as Methylene Blue and ICG. These agents have already been approved for use in the clinic, whereas targeted probes have yet to see regulatory approval [98]. Despite the significant barriers to implementation of the EPR effect as a delivery strategy for FIGS, current research has validated the potential for strategic improvements and clinical translation of utilizing the effect.

## Tumor Targeting Strategies – Active

The strategy of active targeting in FIGS is based on the recognition of a fluorescent moiety conjugated ligand by its target receptor on a tumor. This technique harnesses the unique microenvironment of a tumor, focusing on using ligands to target differentially expressed proteins in tumors for increased, and more precise contrast agent delivery. The accessibility of the tumor receptor and its level of expression are important factors to consider in active targeting. Ligands used to target the overexpressed receptor on the tumor should have a high binding affinity and low toxicity, exhibit high specificity, and present groups for conjugation to a contrast agent for imaging [99]. As shown in Fig. 3, antibodies, antibody fragments, proteins, peptides, aptamers, small molecules, and nanoparticles are examples of commonly used ligands used to target tumor receptors for FIGS. While active targeting probes may achieve a higher degree of specificity for the tumor target than passive targeting, background noise and non-specific binding still occur, suggesting the need for further improvement. High background noise and non-specific binding can significantly limit the detection capabilities of FIGS, inhibiting the surgeon's ability to differentiate cancerous tissue and metastatic lesions. The pharmacokinetic properties of the probe are a contributing factor to the background noise and non-specific binding. Many dyes that are used for FIGS are cleared from the body through the liver, which can result in a high level of background signal in the gastrointestinal tract. Further investigations to reduce background noise, as well as non-specific binding, are important for improving the accuracy and signal of FIGS [100]. Finally, one of the biggest limitations of FIGS is that it lacks the ability to image preoperatively in most cases, and it cannot image at all clinically relevant depths. It is essential to continue developing active targeting methods that can functionally integrate preoperative and intraoperative imaging, as well improve the SBR for FIGS.

### Antibodies and Antibody Derivatives

The use of antibodies as a FIGS targeting strategy is widely investigated and, while the vast majority of these investigations for FIGS are pre-clinical, several antibody-fluorophore conjugates are in clinical trials [101–104]. Cetuximab and Panitumumab, targeting human epidermal growth factor receptor (EGFR), and Bevacizumab, targeting vascular endothelial growth factor (VEGF), are common antibodies used for fluorescence imaging in current clinical trials for a variety of different cancers ([NCT02583568](#), [NCT02415881](#), [NCT03134846](#)) [57, 105]. In addition to imaging, antibodies have the potential to be a useful tool for diagnostics, therapeutics, and drug delivery. However, the pharmacokinetic

requirements differ for each of these uses [106, 107]. For instance, slow circulation is preferential for therapeutic antibodies, but fast clearance is necessary for imaging purposes. Therefore, dual function antibody probes must balance the requirements for its desired function. The binding sites of antibodies can be modified to achieve high specificity for a given target, a favorable trait for an imaging agent. However, antibodies have limitations in FIGS. This is in part due to their large size (~150 kDa) and long circulation time, resulting in impaired tumor penetration and increased background signal during imaging. Engineered antibody fragments provide a compromise to full antibodies. Fragments are smaller in size (25–100 kDa), and therefore have faster clearance and decreased background signal during imaging, but sacrifice the extent of tumor uptake. These fragments have shown efficacy in recent studies of prostate cancer [108, 109]. Nanobodies and affibodies have also shown efficacy as alternatives to full antibodies. Affibodies, tiny protein scaffolds, are an advantageous alternative to full antibodies because of their small size (2–20 kDa) which allows for deeper tissue penetration, as well as their fast circulation time. These characteristics in addition to their cheaper cost, make affibodies an excellent candidate for imaging [110, 111]. An IRDye800CW labeled synthetic affibody, ABY-029, has recently demonstrated success in preclinical studies for labeling EGFR positive regions in gliomas, and is currently undergoing microdosing clinical trials for multiple cancer types [112, 113]. Nanobodies (~12–15kDa) are typically constructed from the variable region of an antibody's heavy chain. The advantages of nanobodies are similar to affibodies in many regards, featuring high penetration and targeting, and rapid clearance [114, 115]. Recent trends in antibody-based targeting strategies for FIGS may favor the smaller fragments and derivatives of antibodies rather than their fully assembled parents, because of their increased compatibility with imaging requirements.

## Peptides

Peptides are linear or cyclic amino acid chains linked by peptide bonds. This type of probe is advantageous as an imaging agent because of rapid distribution, small size, ease and scalability of synthesis, specificity, and stability [116]. Despite their many advantages, peptides must be optimized in order to demonstrate translational potential. Their short half-life and degradation may prevent peptides from reaching their target. To combat this, peptides can be chemically modified to slow renal clearance and increase target affinity. Methods for modifying peptide probes for FIGS has been previously described [117]. There are a wide variety of peptides being investigated in laboratory settings including Arg-Gly-Asp (RGD), Somatostatin (SST), Gastrin releasing peptide (GRP) and Neurotensin (NT) among many others. In a recent study, a cyclic RGD-ZW800–1 was investigated as a generic tracer for multiple cancer types, and proved to be efficacious for both tumor and ureter identification [118]. The use of a zwitterionic dye such as ZW800 can overcome problems with background noise in FIGS. Because this dye is eliminated through renal filtration rather than liver clearance, studies have shown improved SBR and decreased background noise, especially in the gastrointestinal tract [100, 119] Neurotensin conjugated to IRDye800 also showed value as a fluorescence imaging agent for potential use in screening pancreatic cancer patients [120]. Another peptide probe of recent interest is the pHLIP derived probe, or the pH low insertion peptide probe. This targeting strategy utilizes the characteristic acidic pH found in the tumor environment. The probe is designed so that upon sensing a

change in pH, the probe is protonated and becomes more hydrophobic, thus folding and forming a transmembrane helix inserted in the membrane of the cancerous cells [121].

Recent studies have employed this technology for detecting bladder cancer and improving fluorescence signal in a breast cancer model [122, 123].

## Aptamers

Aptamers are single stranded DNA or RNA sequences that are capable of binding to targets by forming three-dimensional structures. Aptamers are typically selected *in vitro* using a method called systematic evolution of ligands by exponential enrichment (SELEX), as well as variations on this technology. Explanations of aptamer selection using these libraries have been previously described [124, 125]. Aptamers have shown great potential for serving as a targeted probe for FIGS imaging because of the small size (5–40 kDa), ease of synthesis and modification, wide range of targets, and stability. Drawbacks to using these sequences as targeting agents for FIGS are that aptamers are regularly degraded by nucleases, and not all aptamers have a high binding affinity. This can result in weak signal generation for imaging. However, this can be improved upon by using scaffolds, such as nanoparticles or quantum dots, to improve the binding affinity of the aptamer, thus providing increased specificity and enhanced signal [126]. A recent study demonstrated the efficacy of aptamer conjugated quantum dots for identifying margins in glioma by binding to EGFR variant III on the tumor cell surface [127]. A different study employed the use of silica based nanoparticle and aptamer conjugate to act as a theranostic agent to image and inhibit tumor angiogenesis [128]. Beyond FIGS, aptamers have shown great potential for use in a variety of applications, especially in drug delivery. Aptamers are prevalent in clinical trials, but not yet in relation to FIGS. Most of the current clinical trials investigate aptamer use in macular degeneration, though recently posted clinical trials propose identifying aptamers to identify biomarkers in bladder cancer ([NCT02957370](#)), as well as using a Ga-68 aptamer conjugate to test its diagnostic capabilities in positron emission tomography (PET)/CT ([NCT03385148](#)).

## Ligand Based targeting

There are several ligand-based targeting strategies that are typically used to functionalize and specialize the surface of nanoparticles. Two commonly explored examples of this strategy include proteins like transferrin, and small molecules such as folic acid. Small molecules are advantageous as a targeting strategy because of their size, cost, and stability. However, they are scarce because of the difficulty of finding a ligand, and the intense screening process involved [72, 129]. These molecules are typically used to functionalize the surface of nanoparticles for more specific targeting. Folic acid is perhaps the most common example of a small molecule used in the literature. Folic acid conjugated quantum dots has proved successful as a theranostic agent in human cervical carcinoma cells [130]. Additionally, OTL38 a folate receptor targeted contrast agent has shown success in multiple cancer models [131, 132]. A recent study used a folate targeted contrast agent to identify lung cancer in large animal models [133]. Protein ligand-based strategies, such as transferrin, are advantageous in their specificity, but present problems because of bulk and

ability to trigger an immune response. A recent study implicated the use of holo-transferrin ICG nanoassemblies for imaging and photothermal therapy in gliomas [134].

### Improving Active Targeting

Despite the wide variety of targeting ligands explored in pre-clinical studies, there are still many limitations to active targeting for FIGS. While active targeting exhibits increased specificity of the probe for its target, non-specific binding still occurs, as shown in Fig. 3. Active probes constantly emit fluorescence with excitation, regardless of their proximity to the target, producing elevated background noise in FIGS [135, 136]. Additionally, off-target binding can occur if the targeted receptor is expressed in non-cancerous tissues. While each type of targeting strategy has its own strengths and weaknesses, there are several widely adapted strategies to improve the efficacy of these probes, including the use of nanoparticles and activatable probes. Nanoparticles may play a significant role in FIGS, especially in acting as a scaffolding system for many of the aforementioned targeting strategies. The large surface area to volume ratio of nanoparticles provides a large area to attach a wide range of targeting moieties. However, the long-term effects of nanoparticle administration are still not fully understood. Biocompatibility, biodegradability and toxicity properties must be carefully considered on a case to case basis [137]. Nanoparticle size, shape, charge, and hydrophobicity can all influence the conjugation with a ligand [72]. Using a nanoparticle as a scaffold for a targeting ligand allows for multiple interactions, and thus increased specificity with the target. Nanoparticle entrapped dyes have shown enhanced fluorescence and tumor contrast, and nanoparticles are effective carriers for drug delivery [53]. Previous studies have also shown that careful modification of nanoparticle size and surface coating can alter their biodistribution to favor renal filtration, allowing for increased SBR and decreased background noise [138]. Further investigation of nanoparticle modifications to alter the pharmacokinetic properties has the potential to improve the detection capabilities of FIGS. Given their functionality, current research for FIGS has demonstrated increased use of nanoparticles for more effective delivery, as well as brighter contrast.

There are two main categories of active targeting probes: 'always on' probes, and 'activatable' probes. Activatable probes offer several advantages over probes that are always on, such as higher contrast, lower background noise, and improved sensitivity. As shown in Fig. 3, the fluorescent properties of these probes remain quiescent until they receive a signal to fluoresce, such as enzymatic cleavage or cellular internalization. Probes such as these that are activated by biomolecules in the local tumor environment have the potential to overcome some of the pitfalls of FIGS, such as background noise and low SBR, by eliminating non-specific binding and subsequent off-target fluorescence. Difficulties with implementation of these probe types depend on the specifics of the probe. High molecular weight activatable probes cannot be sprayed onto the surface of the tumor, and must be injected intravenously. It may take days for the necessary tumor to background ratio to be achieved. Molecular binding-based activatable probes are typically conjugated to an antibody and are therefore significantly large in size. However, enzymatic activity controlled probes can be small in size, and therefore some can be applied with a spray [135]. The use of a matrix metalloprotease, and  $\gamma$ -glutamyltranspeptidase as agents for inducing probe enzymatic cleavage and activating fluorescence have been recently explored for cancer detection [139].

Many of the aforementioned active targeting mechanisms have potential applications in the field of drug delivery, as well as FIGS. For instance, antibody drug conjugates are being utilized in both preclinical studies as well as early and late stage clinical trials. These studies have shown increased ability to target diseased cells, and increased antitumor potency [140–143]. Peptide and aptamer based delivery systems have also shown efficacy in reducing off-target effects and increasing drug delivery to the tumor [144–146]. Therefore there is an opportunity for parallel development of imaging probes and drug delivery systems that target the same receptor or biomarker. Furthermore, there is an opportunity to improve active targeting by incorporating multimodality imaging probes. One of the biggest limitations with FIGS is that it can only be used intraoperatively, and cannot be used for preoperative planning. However multimodal active targeting probes that use FIGS in conjunction with MRI, PET, photoacoustic imaging, or CT can potentially improve preoperative detection, and intraoperative resection [147–155]. Current multimodal probes employ many of the active targeting strategies to achieve a high level of accuracy for probe delivery, and overcome some of the limitations of single modality active targeting.

While the variety of targeted probes continues to expand in versatility and function, regulatory restrictions are a significant consideration to successful implementation into clinical settings. In addition, each type of probe comes with its own set of developmental difficulties. Given the wide successes of different types of probes in the laboratory, it seems that there is not one type of probe that exceeds all others in terms of clinical potential. Instead, the functional imaging and targeting requirements should dictate the type of probe used, as each carry its own advantages. Further toxicity and feasibility studies, as well as appearance in clinical trials are needed to progress targeted probes for FIGS into the clinic.

### ***In Vivo* vs. *Ex Vivo* Imaging**

Surgical resection of tumors typically consists of three components. The primary tumor is assessed before the initial resection, the surgical margin is analyzed for remaining tumor, and the surgical field is assessed for regional metastasis [156]. As mentioned previously, remaining tumor at the surgical margin can result in disease recurrence. There are several strategies available to analyze the surgical margin for the presence of microscopic disease to achieve negative margins. Two common methods for intraoperative pathological examination of the surgical margin include intraoperative frozen section analysis (IFSA) and imprint cytology. Both methods have demonstrated reduced rates of positive margins after surgery, but the technology has limitations. IFSA, the current gold standard in margin detection, is highly variable in terms of sensitivity, and requires confirmation of negative margins on multiple tissue samples by a pathologist, which can add significant time onto the surgical procedure [157–159]. Imprint cytology is a faster and more cost effective method of analysis in comparison to IFSA. However, it also has variable levels of sensitivity, and has a high probability of false-negative results [160]. The use of fluorescence imaging is increasingly being considered as an alternative method of histological analysis. Typically, FIGS is associated with intravenous administration of contrast agents for tumor detection, as the advantages of intraoperative real-time feedback of the surgical field are evident. However, significant investigations of fluorescent probe toxicity, dosage, optimal imaging time, and accuracy of molecular targeting must be conducted and approved before this

technology can become the standard of care for eligible cancer patients. As an alternative use of FIGS, recent studies have demonstrated the use of *ex vivo* contrast agent administration to perform real-time fluorescence guided histology [36, 161–163]. This technique lacks some of the intraoperative advantages such as preventing excessive tissue resection, but avoids some of the rigorous regulatory approval and testing, while still providing critical feedback on margin and nodal status. *Ex vivo* techniques are particularly useful for sentinel lymph node and positive margin detection. This strategy is efficacious, and avoids extended operating time and potentially re-excision. A recent study employed dual probe difference specimen imaging to differentiate between tumor and benign tissue using both a targeted and a non-targeted probe, as shown in Figure 4 [161]. *Ex vivo* analysis provides an opportunity to utilize many of the targeted probes being developed in the labs into the clinic without extensive regulatory hurdles.

## Clinical Translation

The number of new clinical trials involving FIGS has increased dramatically over the past decade [164]. The adoption of target-specific probes and NIR dyes requires strict regulatory review to ensure patient safety. To fulfill these regulatory requirements, many current clinical trials are centralized around investigating the safety and efficacy of the FIGS agents. Endpoints to developing successful contrast agents, devices, and procedures need to be well-defined in order to see faster progress of FIGS into patient care [165]. Current clinical trials for FIGS vary widely in terms of contrast agent, device, ligand conjugation, and objective, as shown in Table 2. ICG remains the most prominent contrast agent used in clinical trials, which is unsurprising due to its low toxicity and current FDA approval status. ICG is also significantly less expensive than other available contrast agents. SLN detection is currently under investigation for many cancer types, and there are some intriguing implementations of new technology. For example, in a fluorescence imaging study for SLN detection in head and neck cancer, the use of a hands free goggle system is being explored as an alternative to traditional monitor display FIGS devices as shown in Fig. 5 (NCT03297957) [166, 167]. IRDye800 has become another prominent contrast agent on the clinical trial stage. Many studies utilizing IRDye800 are investigating dosage, safety, and efficacy (NCT03384238, NCT02901925, NCT02497599). This dye is used in conjugation with several different antibodies across the spectrum of clinical trials, allowing for theoretically more precise tumor localization. Besides antibody conjugated IRDye800, there are several clinical trials studying IRDye800 conjugated to peptides. Recently a synthetic protease activated peptide dye conjugate entitled AVB-620, has entered a phase 2 trial for tumor and lymph node detection. Additionally, an anti-EGFR IRDye800 labeled affibody peptide has entered a phase 0 trial microdose study for signal detection in patients with recurrent gliomas (NCT02901925). In addition to ICG, IRDye800, and 5-ALA fluorescent dye based imaging agents in clinical trials, several other investigational probes have shown potential as prominent candidates for FIGS and cancer detection. The folate-receptor targeted fluorescent moiety, OTL38, has become a successful active targeting probe in clinical trials. A phase 2 study is currently underway, to investigate the ability of this imaging probe to aid in the detection of pulmonary nodules, as well as study the safety and tolerability of a single dose of this imaging agent (NCT02872701). The OTL38 probe is also being investigated in

a phase 3 study to detect folate receptor positive lesions in ovarian cancer during cytoreduction, interval debulking, or recurrent ovarian cancer surgery (NCT03180307). Surgimab, (SGM-101) a fluorescent anti-carcinoembryonic (CEA) monoclonal antibody is another promising FIGS probe in phase 1 and 2 clinical trials. This probe is currently being investigated for safety and performance in patients with cancer of the colon, rectum or pancreas (NCT02973672). Results from this study suggested that the SGM-101 probe was safe and efficacious in detecting cancer [168]. A recently completed clinical trial investigated the ability of the LUM imaging system and the LUM015 to detect residual breast cancer and reduce positive margins (NCT02438358). The LUM015 probe contains a Cy5 fluorophore linked to a cathepsin activatable peptide. This probe and the LUM imaging system are in several upcoming and currently recruiting clinical trials including a phase C clinical trial for residual breast cancer (NCT03321929), a phase ½ study for detection of gastrointestinal cancers (NCT02584244) and a feasibility study for detection of prostate cancer (NCT03441464). The significant increase in clinical trials for FIGS suggests the potential for more rapid regulatory approval and clinical implementation in the future.

## Opportunities in Image-Guided Surgery

FIGS has emerged as an imaging technology with significant potential for clinical efficacy, especially in the field of surgical oncology. Despite its progress, there are still many opportunities for growth in the field. Given below are a few potential examples:

- **Multimodal imaging:** Using a combination of several imaging modalities to diagnose a patient increases diagnostic accuracy. Several recent studies investigated the use of targeted nanoparticles for MRI and FIGS, providing the surgeon concurrence between preoperative planning and intraoperative resection [169, 170]. Combining photoacoustic imaging with FIGS is another area of interest for multimodal imaging [171]. It has been demonstrated that the use of multiple imaging modalities has a synergistic effect on the ability to detect and differentiate cancer both preoperatively and intraoperatively [172].
- **Photodynamic therapy:** FIGS has theranostic capabilities, especially with using NIR contrast agents to induce an immune, chemical, or thermal response in cancer cells. Recent photoimmunotherapy to induce immunogenic cell death with an antibody-conjugated NIR dye has demonstrated an interesting theranostic path to further investigate [173, 174]. Moreover, early studies have begun to explore photodynamic therapy and photothermal therapy as combined imaging and therapy strategies for cancer treatment [175, 176] (Fig. 6).
- **NIR II window:** Typical NIR probes fall in the range of 700–1000 nm, whereas NIR-II agents emit in the 1000–1700 nm range. This shift in emission spectra has demonstrated deeper light penetration depths as well as higher contrast. These preliminary successes suggest a need for further NIR-II probe development [177, 178].
- **Nanotechnology:** Nanotechnology continues to play a key role in FIGS, and offers significant opportunities in terms of conjugation, targeting, and dye encapsulation for enhanced FIGS and multimodality performance. Current

research has begun to explore the use of biodegradable nanoparticles for imaging and therapy in cancer treatment [179, 180]. Success in these experiments tackles the concern of toxicity of non-biodegradable nanoparticles, strengthening their potential for translation. [150, 151].

- **Refinement of Imaging Probes:** Further refinement of contrast agents and bulky passive, active, and activatable probes for FIGS is essential to provide the precision and clarity necessary for clinical translation.
- **Applications in advanced cancer models:** In order to apply FIGS technology to highly metastatic and advanced cancers like pancreatic and ovarian, the discovery of early detection biomarkers to target is of utmost importance. Furthermore, the use of large animal models and comparative studies on companion animals as part of standard veterinary treatment may be beneficial.

As FIGS technology progresses, so does the conversation of surgical resection in surgical oncology. In the interest of providing the most comprehensive and precise patient care, FIGS may eventually align with the implementation of highly personalized medicine. The future of FIGS may involve isolating specific cancer biomarkers for a patient, and selecting the corresponding targeted fluorescence probe that would most effectively detect their cancer and metastases. Increased probe specificity and functionality would allow for more complete and thus potentially curative surgical resections for many cancer types. Though many opportunities for growth in the field still exist, FIGS has the potential for widespread implementation as a critical tool for improving surgical resection of cancer.

## Acknowledgements:

This work was supported in part by the National Institutes of Health [grant numbers R01EB019449, R00CA153916, P20 GM103480, and P30CA036727 (Fred and Pamela Buffett Cancer Center at UNMC)], the Nebraska Cattlemen's Ball Development Fund, and the Nebraska Research Initiative.

## References

1. Stewart B, Wild C (2014) World cancer report 2014. International Agency for Research on Cancer
2. Siegel RL, Miller KD, Jemal A (2018) Cancer statistics, 2018. *CA Cancer J Clin* 68:7–30 [PubMed: 29313949]
3. Orosco RK, Tsien RY, Nguyen QT (2013) Fluorescence imaging in surgery. *IEEE Rev Biomed Eng* 6:178–87 [PubMed: 23335674]
4. Nguyen QT, Tsien RY (2013) Fluorescence-guided surgery with live molecular navigation — a new cutting edge. *Nat Rev Cancer* 13:653–662 [PubMed: 23924645]
5. Keating J, Tchou J, Okusanya O, et al. (2016) Identification of breast cancer margins using intraoperative near-infrared imaging. *J Surg Oncol* 113:508–514 [PubMed: 26843131]
6. Madajewski B, Judy BF, Mouchli A, et al. (2012) Intraoperative near-infrared imaging of surgical wounds after tumor resections can detect residual disease. *Clin Cancer Res* 18:5741–51 [PubMed: 22932668]
7. Narod S (2016) Can advanced-stage ovarian cancer be cured? *Nat Rev Clin Oncol* 13:255–261 [PubMed: 26787282]
8. Witkowski ER, Smith JK, Tseng JF (2013) Outcomes following resection of pancreatic cancer. *J Surg Oncol* 107:97–103 [PubMed: 22991309]

9. Shaib Y, Davila J, Naumann C, El-Serag H (2007) The Impact of Curative Intent Surgery on the Survival of Pancreatic Cancer Patients: A U.S. Population-Based Study. *Am J Gastroenterol* 102:1377–1382 [PubMed: 17403071]
10. Rossi ML, Rehman AA, Gondi CS (2014) Therapeutic options for the management of pancreatic cancer. *World J Gastroenterol* 20:11142–11159 [PubMed: 25170201]
11. Tamburrino D, Partelli S, Crippa S, et al. (2014) Selection criteria in resectable pancreatic cancer: a biological and morphological approach. *World J Gastroenterol* 20:11210–5 [PubMed: 25170205]
12. Hidalgo M (2010) Pancreatic Cancer. *N Engl J Med* 362:1605–1617 [PubMed: 20427809]
13. Nick AM, Coleman RL, Ramirez PT, Sood AK (2015) A framework for a personalized surgical approach to ovarian cancer. *Nat Rev Clin Oncol* 12:239–245 [PubMed: 25707631]
14. Sehouli J, Grabowski JP (2017) Surgery for recurrent ovarian cancer: Options and limits. *Best Pract Res Clin Obstet Gynaecol* 41:88–95 [PubMed: 27865654]
15. Liberale G, Vankerckhove S, Gomez Caldon M, et al. (2016) Fluorescence imaging after indocyanine green injection for detection of peritoneal metastases in patients undergoing cytoreductive surgery for peritoneal carcinomatosis from colorectal cancer: A pilot study. *Ann Surg* 264:1110–1115 [PubMed: 27828822]
16. Hoogstins CE, Weixler B, Boogerd LS, et al. (2017) In Search for Optimal Targets for Intraoperative Fluorescence Imaging of Peritoneal Metastasis From Colorectal Cancer. *Biomark Cancer* 9:1179299X1772825
17. Barth CW, Gibbs SL (2017) Direct administration of nerve-specific contrast to improve nerve sparing radical prostatectomy. *Theranostics* 7:573–593 [PubMed: 28255352]
18. Gibbs-Strauss SL, Nasr K, Fish KM, et al. (2011) Nerve-Highlighting Fluorescent Contrast Agents for Image-Guided Surgery. *Mol Imaging* 10:91–101 [PubMed: 21439254]
19. Hussain T, Mastrodimos MB, Raju SC, et al. (2015) Fluorescently labeled peptide increases identification of degenerated facial nerve branches during surgery and improves functional outcome. *PLoS One* 10:e0119600
20. Hussain T, Nguyen LT, Whitney M, et al. (2016) Improved facial nerve identification during parotidectomy with fluorescently labeled peptide. *Laryngoscope* 126:2711–2717 [PubMed: 27171862]
21. Whitney MA, Crisp JL, Nguyen LT, et al. (2011) Fluorescent peptides highlight peripheral nerves during surgery in mice. *Nat Biotechnol* 29:352–356 [PubMed: 21297616]
22. He K, Zhou J, Yang F, et al. (2018) Near-infrared Intraoperative Imaging of Thoracic Sympathetic Nerves: From Preclinical Study to Clinical Trial. *Theranostics* 8:304–313 [PubMed: 29290809]
23. Hong G, Antaris AL, Dai H (2017) Near-infrared fluorophores for biomedical imaging. *Nat Biomed Eng* 1:10
24. Moore GE, Peyton WT, French LA, Walker WW (1948) The Clinical Use of Fluorescein in Neurosurgery. *J Neurosurg* 5:392–398 [PubMed: 18872412]
25. Dilek O, Ihsan A, Tulay H (2011) Anaphylactic reaction after fluorescein sodium administration during intracranial surgery. *J Clin Neurosci* 18:430–1 [PubMed: 21237654]
26. Tanahashi S (1995) An Anaphylactoid Reaction After Administration of Fluorescein Sodium During Neurosurgery. *Can J Anaesth* 42:181–5 [PubMed: 7743565]
27. Mondal SB, Gao S, Zhu N, et al. (2014) Real-time Fluorescence Image-Guided Oncologic Surgery. *Adv Cancer Res* 124:171–211 [PubMed: 25287689]
28. Thevarajah S, Huston TL, Simmons RM (2005) A comparison of the adverse reactions associated with isosulfan blue versus methylene blue dye in sentinel lymph node biopsy for breast cancer. *Am J Surg* 189:236–9 [PubMed: 15720998]
29. Kidd SA, Lancaster PAL, Anderson JC, et al. (1996) Fetal Death After Exposure to Methylene Blue Dye During Mid-Trimester Amniocentesis in Twin Pregnancy. *Prenat Diagn* 16:39–47 [PubMed: 8821851]
30. Zhang RR, Schroeder AB, Grudzinski JJ, et al. (2017) Beyond the margins: real-time detection of cancer using targeted fluorophores. *Nat Rev Clin Oncol* 14:347–364 [PubMed: 28094261]

31. Verbeek FPR, van der Vorst JR, Schaafsma BE, et al. (2013) Intraoperative near infrared fluorescence guided identification of the ureters using low dose methylene blue: a first in human experience. *J Urol* 190:574–9 [PubMed: 23466242]
32. Dip FD, Moreira Grecco AD, Nguyen D, et al. (2015) Ureter Identification Using Methylene Blue and Fluorescein In: *Fluorescence Imaging for Surgeons*. Springer International Publishing, Cham, pp 327–332
33. Seif C, Martínez Portillo FJ, Osmonov DK, et al. (2004) Methylene blue staining for nerve-sparing operative procedures: An animal model. *Urology* 63:1205–1208 [PubMed: 15183990]
34. Osorio JA, Breshears JD, Arnaout O, et al. (2015) Ultrasound-guided percutaneous injection of methylene blue to identify nerve pathology and guide surgery. *Neurosurg Focus* 39:E2
35. Candell L, Campbell MJ, Shen WT, et al. (2014) Ultrasound-Guided Methylene Blue Dye Injection for Parathyroid Localization in the Reoperative Neck. *World J Surg* 38:88–91 [PubMed: 24132819]
36. Kir G, Alimoglu O, Sarbay BC, Bas G (2014) Ex vivo intra-arterial methylene blue injection in the operation theater may improve the detection of lymph node metastases in colorectal cancer. *Pathol Res Pract* 210:818–821 [PubMed: 25282546]
37. Tummers QRJG, Schepers A, Hamming JF, et al. (2015) Intraoperative guidance in parathyroid surgery using near-infrared fluorescence imaging and low-dose Methylene Blue. *Surgery* 158:1323–1330 [PubMed: 25958068]
38. van der Vorst JR, Schaafsma BE, Verbeek FPR, et al. (2014) Intraoperative near-infrared fluorescence imaging of parathyroid adenomas with use of low-dose methylene blue. *Head Neck* 36:853–8 [PubMed: 23720199]
39. van der Vorst JR, Vahrmeijer AL, Hutteman M, et al. (2012) Near-infrared fluorescence imaging of a solitary fibrous tumor of the pancreas using methylene blue. *World J Gastrointest Surg* 4:180–4 [PubMed: 22905287]
40. Chu M, Wan Y (2009) Sentinel lymph node mapping using near-infrared fluorescent methylene blue. *J Biosci Bioeng* 107:455–459 [PubMed: 19332308]
41. Ferraro N, Barbarite E, Albert TR, et al. (2016) The role of 5-aminolevulinic acid in brain tumor surgery: a systematic review. *Neurosurg Rev* 39:545–555 [PubMed: 26815631]
42. Zhao S, Wu J, Wang C, et al. (2013) Intraoperative Fluorescence-Guided Resection of High-Grade Malignant Gliomas Using 5-Aminolevulinic Acid-Induced Porphyrins: A Systematic Review and Meta-Analysis of Prospective Studies. *PLoS One* 8:e63682
43. Hadjipanayis CG, Widhalm G, Stummer W (2015) What is the Surgical Benefit of Utilizing 5-Aminolevulinic Acid for Fluorescence-Guided Surgery of Malignant Gliomas? *Neurosurgery* 77:663–73 [PubMed: 26308630]
44. Moiyadi A, Syed P, Srivastava S (2014) Fluorescence-guided surgery of malignant gliomas based on 5-aminolevulinic acid: paradigm shifts but not a panacea. *Nat Rev Cancer* 14:146–146
45. Stummer W, Novotny A, Stepp H, et al. (2000) Fluorescence-guided resection of glioblastoma multiforme utilizing 5-ALA-induced porphyrins: a prospective study in 52 consecutive patients. *J Neurosurg* 93:1003–1013 [PubMed: 11117842]
46. Stummer W, Tonn J- C, Goetz C, et al. (2014) 5-Aminolevulinic acid-derived tumor fluorescence: the diagnostic accuracy of visible fluorescence qualities as corroborated by spectrometry and histology and postoperative imaging. *Neurosurgery* 74:310–9-20
47. Schaafsma BE, Mieog JSD, Hutteman M, et al. (2011) The clinical use of indocyanine green as a near-infrared fluorescent contrast agent for image-guided oncologic surgery. *J Surg Oncol* 104:323–332 [PubMed: 21495033]
48. Marshall M V, Rasmussen JC, Tan I- C, et al. (2010) Near-Infrared Fluorescence Imaging in Humans with Indocyanine Green: A Review and Update. *Open Surg Oncol J* 2:12–25 [PubMed: 22924087]
49. Namikawa T, Sato T, Hanazaki K (2015) Recent advances in near-infrared fluorescence-guided imaging surgery using indocyanine green. *Surg Today* 45:1467–1474 [PubMed: 25820596]
50. Pitsinis V, Provenzano E, Kaklamanis L, et al. (2015) Indocyanine green fluorescence mapping for sentinel lymph node biopsy in early breast cancer. *Surg Oncol* 24:375–379 [PubMed: 26555151]

51. Sugie T, Kassim KA, Takeuchi M, et al. (2010) A novel method for sentinel lymph node biopsy by indocyanine green fluorescence technique in breast cancer. *Cancers (Basel)* 2:713–20 [PubMed: 24281090]
52. Vahrmeijer AL, Hutteman M, van der Vorst JR, et al. (2013) Image-guided cancer surgery using near-infrared fluorescence. *Nat Rev Clin Oncol* 10:507–18 [PubMed: 23881033]
53. Hill TK, Abdulahad A, Kelkar SS, et al. (2015) Indocyanine Green-Loaded Nanoparticles for Image-Guided Tumor Surgery. *Bioconjug Chem* 26:294–303 [PubMed: 25565445]
54. Kraft JC, Ho RJY (2014) Interactions of Indocyanine Green and Lipid in Enhancing Near-Infrared Fluorescence Properties: The Basis for Near-Infrared Imaging in Vivo. *Biochemistry* 53:1275–1283 [PubMed: 24512123]
55. Moore LS, Rosenthal EL, Chung TK, et al. (2017) Characterizing the Utility and Limitations of Repurposing an Open-Field Optical Imaging Device for Fluorescence-Guided Surgery in Head and Neck Cancer Patients. *J Nucl Med* 58:246–251 [PubMed: 27587708]
56. Korb ML, Hartman YE, Kovar J, et al. (2014) Use of monoclonal antibody-IRDye800CW bioconjugates in the resection of breast cancer HHS Public Access. *J Surg Res J Surg Res May* 111:119–128
57. Rosenthal EL, Warram JM, de Boer E, et al. (2015) Safety and Tumor Specificity of Cetuximab-IRDye800 for Surgical Navigation in Head and Neck Cancer. *Clin Cancer Res* 21:3658–66 [PubMed: 25904751]
58. Lu Y, Su Y, Zhou Y, et al. (2013) In vivo behavior of near infrared-emitting quantum dots. doi: 10.1016/j.biomaterials.2013.02.054
59. Luo S, Zhang E, Su Y, et al. (2011) A review of NIR dyes in cancer targeting and imaging. *Biomaterials* 32:7127–7138 [PubMed: 21724249]
60. Ji X, Peng F, Zhong Y, et al. (2014) Fluorescent quantum dots: Synthesis, biomedical optical imaging, and biosafety assessment. *Colloids Surfaces B Biointerfaces* 124:132–139 [PubMed: 25224376]
61. Smith AM, Duan H, Mohs AM, Nie S (2008) Bioconjugated quantum dots for in vivo molecular and cellular imaging. *Adv Drug Deliv Rev* 60:1226–1240 [PubMed: 18495291]
62. Tansi FL, R ger R, Rabenhold M, et al. (2015) Fluorescence-quenching of a liposomal-encapsulated near-infrared fluorophore as a tool for in vivo optical imaging. *J Vis Exp* e52136
63. Lisy M- R, Goermar A, Thomas C, et al. (2008) In Vivo Near-infrared Fluorescence Imaging of Carcinoembryonic Antigen-expressing Tumor Cells in Mice. *Radiology* 247:779–787 [PubMed: 18413884]
64. Pauli J, Brehm R, Spieles M, et al. (2010) Novel Fluorophores as Building Blocks for Optical Probes for In Vivo Near Infrared Fluorescence (NIRF) Imaging. *J Fluoresc* 20:681–693 [PubMed: 20213244]
65. Pansare VJ, Hejazi S, Faenza WJ, Prud'homme RK (2012) Review of Long-Wavelength Optical and NIR Imaging Materials: Contrast Agents, Fluorophores, and Multifunctional Nano Carriers. *Chem Mater* 24:812–827 [PubMed: 22919122]
66. Hill TK, Mohs AM (2016) Image-guided tumor surgery: will there be a role for fluorescent nanoparticles? *Wiley Interdiscip Rev Nanomedicine Nanobiotechnology* 8:498–511 [PubMed: 26585556]
67. Gioux S, Kianzad V, Ciocan R, et al. (2009) High-power, computer-controlled, light-emitting diode-based light sources for fluorescence imaging and image-guided surgery. *Mol Imaging* 8:156–65 [PubMed: 19723473]
68. Gioux S, Choi HS, Frangioni J V (2010) Image-Guided Surgery using Invisible Near-Infrared Light: Fundamentals of Clinical Translation. *Mol Imaging* 9:237–255 [PubMed: 20868625]
69. DSouza A V, Lin H, Henderson ER, et al. (2016) Review of fluorescence guided surgery systems: identification of key performance capabilities beyond indocyanine green imaging. *J Biomed Opt* 21:80901 [PubMed: 27533438]
70. Zhu B, Sevic-Muraca EM (2015) A review of performance of near-infrared fluorescence imaging devices used in clinical studies. *Br J Radiol* 88:20140547

71. Matsumura Y, Maeda H, Jain RK, et al. (1986) A new concept for macromolecular therapeutics in cancer chemotherapy: mechanism of tumorotropic accumulation of proteins and the antitumor agent smancs. *Cancer Res* 46:6387–92 [PubMed: 2946403]
72. Bertrand N, Wu J, Xu X, et al. (2014) Cancer nanotechnology: the impact of passive and active targeting in the era of modern cancer biology. *Adv Drug Deliv Rev* 66:2–25 [PubMed: 24270007]
73. Maeda H, Tsukigawa K, Fang J (2016) A Retrospective 30 Years After Discovery of the Enhanced Permeability and Retention Effect of Solid Tumors: Next-Generation Chemotherapeutics and Photodynamic Therapy-Problems, Solutions, and Prospects. *Microcirculation* 23:173–182 [PubMed: 26237291]
74. Kharraishvili G, Simkova D, Bouchalova K, et al. (2014) The role of cancer-associated fibroblasts, solid stress and other microenvironmental factors in tumor progression and therapy resistance. *Cancer Cell Int* 14:41 [PubMed: 24883045]
75. Fang J, Nakamura H, Maeda H (2011) The EPR effect: Unique features of tumor blood vessels for drug delivery, factors involved, and limitations and augmentation of the effect. *Adv. Drug Deliv. Rev.* 63:136–151 [PubMed: 20441782]
76. Carmeliet P, Jain RK (2000) Angiogenesis in cancer and other diseases. *Nature* 407:249 [PubMed: 11001068]
77. Bergers G, Benjamin LE (2003) Angiogenesis: Tumorigenesis and the angiogenic switch. *Nat Rev Cancer* 3:401–410 [PubMed: 12778130]
78. Morikawa S, Baluk P, Kaidoh T, et al. (2002) Abnormalities in pericytes on blood vessels and endothelial sprouts in tumors. *Am J Pathol* 160:985–1000 [PubMed: 11891196]
79. Padera TP, Kadambi A, di Tomaso E, et al. (2002) Lymphatic metastasis in the absence of functional intratumor lymphatics. *Science* 296:1883–6 [PubMed: 11976409]
80. Sriraman SK, Aryasomayajula B, Torchilin VP (2014) Barriers to drug delivery in solid tumors. *Tissue barriers* 2:e29528
81. Maeda H (2012) Macromolecular therapeutics in cancer treatment: The EPR effect and beyond. *J Control Release* 164:138–144 [PubMed: 22595146]
82. Nakamura H, Etrych T, Chytil P, et al. (2014) Two step mechanisms of tumor selective delivery of N-(2-hydroxypropyl)methacrylamide copolymer conjugated with pirarubicin via an acid-cleavable linkage. *J Control Release* 174:81–87 [PubMed: 24269967]
83. Kobayashi H, Watanabe R, Choyke PL (2013) Improving conventional enhanced permeability and retention (EPR) effects; what is the appropriate target? *Theranostics* 4:81–9 [PubMed: 24396516]
84. Nakamura Y, Mochida A, Choyke PL, Kobayashi H (2016) Nanodrug Delivery: Is the Enhanced Permeability and Retention Effect Sufficient for Curing Cancer? *Bioconjug. Chem.* 27:2225–2238 [PubMed: 27547843]
85. Jain RK, Stylianopoulos T (2010) Delivering nanomedicine to solid tumors. *Nat Rev Clin Oncol* 7:653–664 [PubMed: 20838415]
86. Padera TP, Stoll BR, Tooredman JB, et al. (2004) Pathology: Cancer cells compress intratumour vessels. *Nature* 427:695–695 [PubMed: 14973470]
87. Jain RK, Martin JD, Stylianopoulos T (2014) The role of mechanical forces in tumor growth and therapy. *Annu Rev Biomed Eng* 16:321–46 [PubMed: 25014786]
88. Heldin C- H, Rubin K, Pietras K, Östman A (2004) High interstitial fluid pressure — an obstacle in cancer therapy. *Nat Rev Cancer* 4:806–813 [PubMed: 15510161]
89. Baxter LT, Jain RK (1989) Transport of Fluid and Macromolecules in Tumors I. Role of Interstitial Pressure and Convection. *Microvasc Res* 37:77–104 [PubMed: 2646512]
90. Wu M, Frieboes HB, Chaplain MAJ, et al. (2014) The effect of interstitial pressure on therapeutic agent transport: Coupling with the tumor blood and lymphatic vascular systems. *J Theor Biol* 355:194–207 [PubMed: 24751927]
91. Miao L, Lin CM, Huang L (2015) Stromal barriers and strategies for the delivery of nanomedicine to desmoplastic tumors. *J Control Release* 219:192–204 [PubMed: 26277065]
92. May JP, Li S- D (2013) Hyperthermia-induced drug targeting. *Expert Opin Drug Deliv* 10:511–527 [PubMed: 23289519]

93. Durymanov MO, Rosenkranz AA, Sobolev AS (2015) Current Approaches for Improving Intratumoral Accumulation and Distribution of Nanomedicines. *Theranostics* 5:1007–20 [PubMed: 26155316]
94. Ojha T, Pathak V, Shi Y, et al. (2017) Pharmacological and physical vessel modulation strategies to improve EPR-mediated drug targeting to tumors ☆. doi: 10.1016/j.addr.2017.07.007
95. Yokoi K, Tanei T, Godin B, et al. (2014) Serum biomarkers for personalization of nanotherapeutics-based therapy in different tumor and organ microenvironments. *Cancer Lett* 345:48–55 [PubMed: 24370567]
96. Yokoi K, Kojic M, Milosevic M, et al. (2014) Capillary-wall collagen as a biophysical marker of nanotherapeutic permeability into the tumor microenvironment. *Cancer Res* 74:4239–46 [PubMed: 24853545]
97. Bolkestein M, de Blois E, Koelewijn SJ, et al. (2016) Investigation of Factors Determining the Enhanced Permeability and Retention Effect in Subcutaneous Xenografts. *J Nucl Med* 57:601–7 [PubMed: 26719375]
98. Miller J, Wang ST, Orukari I, et al. (2017) Perfusion-based fluorescence imaging method delineates diverse organs and identifies multifocal tumors using generic near infrared molecular probes. *J Biophotonics*. doi: 10.1002/jbio.201700232
99. Srinivasarao M, Galliford C V., Low PS (2015) Principles in the design of ligand-targeted cancer therapeutics and imaging agents. *Nat Rev Drug Discov* 14:203–219 [PubMed: 25698644]
100. Choi HS, Gibbs SL, Lee JH, et al. (2013) Targeted zwitterionic near-infrared fluorophores for improved optical imaging. *Nat Biotechnol* 31:148–153 [PubMed: 23292608]
101. Nagaya T, Nakamura YA, Choyke PL, Kobayashi H (2017) Fluorescence-Guided Surgery. *Front Oncol* 7:314 [PubMed: 29312886]
102. Warram JM, de Boer E, Sorace AG, et al. (2014) Antibody-based imaging strategies for cancer. *Cancer Metastasis Rev* 33:809–22 [PubMed: 24913898]
103. Hiroshima Y, Lwin TM, Murakami T, et al. (2016) Effective fluorescence-guided surgery of liver metastasis using a fluorescent anti-CEA antibody. *J Surg Oncol* 114:951–958 [PubMed: 27696448]
104. Lwin TM, Murakami T, Miyake K, et al. (2018) Tumor-Specific Labeling of Pancreatic Cancer Using a Humanized Anti-CEA Antibody Conjugated to a Near-Infrared Fluorophore. *Ann Surg Oncol* 1–7
105. Moore LS, Rosenthal EL, de Boer E, et al. (2017) Effects of an Unlabeled Loading Dose on Tumor-Specific Uptake of a Fluorescently Labeled Antibody for Optical Surgical Navigation. *Mol Imaging Biol* 19:610–616 [PubMed: 27830425]
106. Freise AC, Wu AM (2015) In vivo imaging with antibodies and engineered fragments. *Mol Immunol* 67:142–52 [PubMed: 25934435]
107. Kobayashi H, Choyke PL, Ogawa M (2016) Monoclonal antibody-based optical molecular imaging probes; considerations and caveats in chemistry, biology and pharmacology. *Curr. Opin. Chem. Biol.* 33:32–38 [PubMed: 27281509]
108. Mazzocco C, Fracasso G, Germain-Genevois C, et al. (2016) In vivo imaging of prostate cancer using an anti-PSMA scFv fragment as a probe. *Sci Rep* 6:23314 [PubMed: 26996325]
109. Sonn GA, Behesnilian AS, Jiang ZK, et al. (2016) Fluorescent Image-Guided Surgery with an Anti-Prostate Stem Cell Antigen (PSCA) Diabody Enables Targeted Resection of Mouse Prostate Cancer Xenografts in Real Time. *Clin Cancer Res* 22:1403–12 [PubMed: 26490315]
110. Owens B (2017) Faster, deeper, smaller—the rise of antibody-like scaffolds. *Nat Biotechnol* 35:602–603 [PubMed: 28700554]
111. Sexton K, Tichauer K, Samkoe KS, et al. (2013) Fluorescent Affibody Peptide Penetration in Glioma Margin Is Superior to Full Antibody. *PLoS One* 8:
112. de Souza ALR, Marra K, Gunn J, et al. (2017) Fluorescent Affibody Molecule Administered In Vivo at a Microdose Level Labels EGFR Expressing Glioma Tumor Regions. *Mol Imaging Biol* 19:41–48 [PubMed: 27379987]
113. Samkoe KS, Gunn JR, Marra K, et al. (2017) Toxicity and Pharmacokinetic Profile for Single-Dose Injection of ABY-029: a Fluorescent Anti-EGFR Synthetic Affibody Molecule for Human Use. *Mol Imaging Biol* 19:512–521 [PubMed: 27909986]

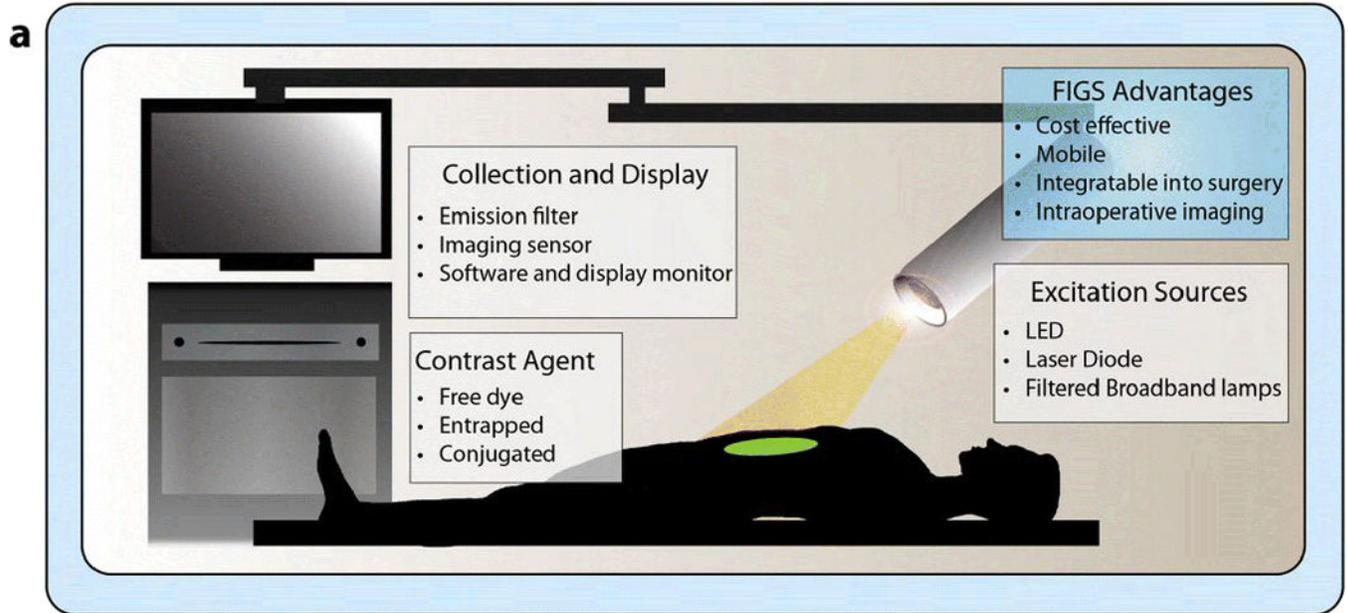
114. Chakravarty R, Goel S, Cai W (2014) Nanobody: the “magic bullet” for molecular imaging? *Theranostics* 4:386–98 [PubMed: 24578722]
115. Debie P, Vanhoeij M, Poortmans N, et al. (2017) Improved Debulking of Peritoneal Tumor Implants by Near-Infrared Fluorescent Nanobody Image Guidance in an Experimental Mouse Model. *Mol Imaging Biol* 1–7
116. Staderini M, Megia-Fernandez A, Dhaliwal K, Bradley M (2017) Peptides for optical medical imaging and steps towards therapy. *Bioorg Med Chem*. doi: 10.1016/J.BMC.2017.09.039
117. Sun X, Li Y, Liu T, et al. (2017) Peptide-based imaging agents for cancer detection. *Adv Drug Deliv Rev* 110–111:38–51
118. Handgraaf HJM, Boonstra MC, Prevoo HAJM, et al. (2017) Real-time near-infrared fluorescence imaging using cRGD-ZW800–1 for intraoperative visualization of multiple cancer types. *Oncotarget* 8:21054–21066 [PubMed: 28416744]
119. Sato K, Gorka AP, Nagaya T, et al. (2016) Role of Fluorophore Charge on the In Vivo Optical Imaging Properties of Near-Infrared Cyanine Dye/Monoclonal Antibody Conjugates. *Bioconjug Chem* 27:404–413 [PubMed: 26444497]
120. Yin X, Wang M, Wang H, et al. (2017) Evaluation of neurotensin receptor 1 as a potential imaging target in pancreatic ductal adenocarcinoma. *Amino Acids* 49:1325–1335 [PubMed: 28536844]
121. Wyatt LC, Lewis JS, Andreev OA, et al. (2017) Applications of pHLIP Technology for Cancer Imaging and Therapy. *Trends Biotechnol* 35:653–664 [PubMed: 28438340]
122. Golijanin J, Amin A, Moshnikova A, et al. (2016) Targeted imaging of urothelium carcinoma in human bladders by an ICG pHLIP peptide ex vivo. *Proc Natl Acad Sci U S A* 113:11829–11834 [PubMed: 27688767]
123. Karabadzhak AG, An M, Yao L, et al. (2014) pHLIP-FIRE, a cell insertion-triggered fluorescent probe for imaging tumors demonstrates targeted cargo delivery in vivo. *ACS Chem Biol* 9:2545–53 [PubMed: 25184440]
124. Darmostuk M, Rimpelova S, Gbelcova H, Ruml T (2015) Current approaches in SELEX: An update to aptamer selection technology. *Biotechnol Adv* 33:1141–1161 [PubMed: 25708387]
125. Hori S, Herrera A, Rossi J, Zhou J (2018) Current Advances in Aptamers for Cancer Diagnosis and Therapy. *Cancers (Basel)* 10:9
126. Huang YF, Chang HT, Tan W (2008) Cancer cell targeting using multiple aptamers conjugated on nanorods. *Anal Chem* 80:567–572 [PubMed: 18166023]
127. Tang J, Huang N, Zhang X, et al. (2017) Aptamer-conjugated PEGylated quantum dots targeting epidermal growth factor receptor variant III for fluorescence imaging of glioma. *Int J Nanomedicine* 12:3899–3911 [PubMed: 28579776]
128. Tan J, Yang N, Zhong L, et al. (2017) A New Theranostic System Based on Endoglin Aptamer Conjugated Fluorescent Silica Nanoparticles. *Theranostics* 7:4862–4876 [PubMed: 29187909]
129. Bazak R, Hourri M, El Achy S, et al. (2015) Cancer active targeting by nanoparticles: a comprehensive review of literature. *J Cancer Res Clin Oncol* 141:769–84 [PubMed: 25005786]
130. Duman FD, Erkisa M, Khodadust R, et al. (2017) Folic acid-conjugated cationic Ag<sub>2</sub>S quantum dots for optical imaging and selective doxorubicin delivery to HeLa cells. *Nanomedicine* 12:2319–2333 [PubMed: 28875744]
131. Predina JD, Newton AD, Connolly C, et al. (2018) Identification of a Folate Receptor-Targeted Near-Infrared Molecular Contrast Agent to Localize Pulmonary Adenocarcinomas. *Mol Ther* 26:390–403 [PubMed: 29241970]
132. Hoogstins CES, Tummers QRJG, Gaarenstroom KN, et al. (2016) A Novel Tumor-Specific Agent for Intraoperative Near-Infrared Fluorescence Imaging: A Translational Study in Healthy Volunteers and Patients with Ovarian Cancer. *Clin Cancer Res* 22:2929–38 [PubMed: 27306792]
133. Keating JJ, Runge JJ, Singhal S, et al. (2017) Intraoperative near-infrared fluorescence imaging targeting folate receptors identifies lung cancer in a large-animal model. *Cancer* 123:1051–1060 [PubMed: 28263385]
134. Zhu M, Sheng Z, Jia Y, et al. (2017) Indocyanine Green-holo-Transferrin Nanoassemblies for Tumor-Targeted Dual-Modal Imaging and Photothermal Therapy of Glioma. *ACS Appl Mater Interfaces* 9:39249–39258 [PubMed: 29039909]

135. Mochida A, Ogata F, Nagaya T, et al. (2018) Activatable fluorescent probes in fluorescence-guided surgery: Practical considerations. *Bioorg Med Chem* 26:925–930 [PubMed: 29242021]
136. Kobayashi H, Choyke PL (2011) Target-Cancer-Cell-Specific Activatable Fluorescence Imaging Probes: Rational Design and in Vivo Applications. *Acc Chem Res* 44:83–90 [PubMed: 21062101]
137. Chinen AB, Guan CM, Ferrer JR, et al. (2015) Nanoparticle Probes for the Detection of Cancer Biomarkers, Cells, and Tissues by Fluorescence. *Chem Rev* 115:10530–10574 [PubMed: 26313138]
138. Choi HS, Liu W, Liu F, et al. (2010) Design considerations for tumour-targeted nanoparticles. *Nat Nanotechnol* 5:42–47 [PubMed: 19893516]
139. Chi C, Zhang Q, Mao Y, et al. (2015) Increased precision of orthotopic and metastatic breast cancer surgery guided by matrix metalloproteinase-activatable near-infrared fluorescence probes. *Sci Rep* 5:14197 [PubMed: 26395067]
140. Alley SC, Okeley NM, Senter PD (2010) Antibody-drug conjugates: targeted drug delivery for cancer. *Curr Opin Chem Biol* 14:529–537 [PubMed: 20643572]
141. Matsuzaki S, Serada S, Hiramatsu K, et al. (2018) Anti-glypican-1 antibody-drug conjugate exhibits potent preclinical antitumor activity against glypican-1 positive uterine cervical cancer. *Int J Cancer* 142:1056–1066 [PubMed: 29055044]
142. Su C- Y, Chen M, Chen L- C, et al. (2018) Bispecific antibodies (anti-mPEG/anti-HER2) for active tumor targeting of docetaxel (DTX)-loaded mPEGylated nanocarriers to enhance the chemotherapeutic efficacy of HER2-overexpressing tumors. *Drug Deliv* 25:1066–1079 [PubMed: 29718725]
143. Semkina AS, Abakumov MA, Skorikov AS, et al. (2018) Multimodal doxorubicin loaded magnetic nanoparticles for VEGF targeted theranostics of breast cancer. *Nanomedicine Nanotechnology, Biol Med*. doi: 10.1016/j.nano.2018.04.019
144. Huang R, Li J, Kebebe D, et al. (2018) Cell penetrating peptides functionalized gambogic acid-nanostructured lipid carrier for cancer treatment. *Drug Deliv* 25:757–765 [PubMed: 29528244]
145. Deshpande P, Jhaveri A, Pattni B, et al. (2018) Transferrin and octaarginine modified dual-functional liposomes with improved cancer cell targeting and enhanced intracellular delivery for the treatment of ovarian cancer. *Drug Deliv* 25:517–532 [PubMed: 29433357]
146. Alibolandani M, Ramezani M, Abnous K, Hadizadeh F (2016) AS1411 Aptamer-Decorated Biodegradable Polyethylene Glycol–Poly(lactic-co-glycolic acid) Nanopolymersomes for the Targeted Delivery of Gemcitabine to Non–Small Cell Lung Cancer In Vitro. *J Pharm Sci* 105:1741–1750 [PubMed: 27039356]
147. Lin R, Huang J, Wang L, et al. (2018) Bevacizumab and near infrared probe conjugated iron oxide nanoparticles for vascular endothelial growth factor targeted MR and optical imaging. *Biomater Sci*. doi: 10.1039/C8BM00225H
148. Rijpkema M, Oyen WJ, Bos D, et al. (2014) SPECT- and fluorescence image-guided surgery using a dual-labeled carcinoembryonic antigen-targeting antibody. *J Nucl Med* 55:1519–24 [PubMed: 24982436]
149. Zhang X- S, Xuan Y, Yang X- Q, et al. (2018) A multifunctional targeting probe with dual-mode imaging and photothermal therapy used in vivo. *J Nanobiotechnology* 16:42 [PubMed: 29673352]
150. Yang H- M, Park CW, Park S, Kim J- D (2018) Cross-linked magnetic nanoparticles with a biocompatible amide bond for cancer-targeted dual optical/magnetic resonance imaging. *Colloids Surfaces B Biointerfaces* 161:183–191 [PubMed: 29080502]
151. Kommidi H, Guo H, Nurili F, et al. (2018) <sup>18</sup>F-Positron Emitting/Trimethine Cyanine-Fluorescent Contrast for Image-Guided Prostate Cancer Management. *J Med Chem* 61:4256–4262 [PubMed: 29676909]
152. Wang X, Yan J, Pan D, et al. (2018) Polyphenol-Poloxamer Self-Assembled Supramolecular Nanoparticles for Tumor NIRF/PET Imaging. *Adv Healthc Mater* 1701505
153. Chi C, Du Y, Ye J, et al. (2014) Intraoperative imaging-guided cancer surgery: from current fluorescence molecular imaging methods to future multi-modality imaging technology. *Theranostics* 4:1072–84 [PubMed: 25250092]

154. Hausner SH, Bauer N, Hu LY, et al. (2015) The Effect of Bi-Terminal PEGylation of an Integrin  $\alpha v \beta_6$  -Targeted  $^{18}\text{F}$  Peptide on Pharmacokinetics and Tumor Uptake. *J Nucl Med* 56:784–90 [PubMed: 25814519]
155. Han Z, Li Y, Roelle S, et al. (2017) Targeted Contrast Agent Specific to an Oncoprotein in Tumor Microenvironment with the Potential for Detection and Risk Stratification of Prostate Cancer with MRI. *Bioconjug Chem* 28:1031–1040 [PubMed: 28201871]
156. Rosenthal EL, Warram JM, Bland KI, Zinn KR (2015) The status of contemporary image-guided modalities in oncologic surgery. *Ann Surg* 261:46–55 [PubMed: 25599326]
157. Kim MJ, Kim CS, Park YS, et al. (2016) The Efficacy of Intraoperative Frozen Section Analysis During Breast-Conserving Surgery for Patients with Ductal Carcinoma In Situ. *Breast Cancer (Auckl)* 10:205–210 [PubMed: 27980416]
158. Ko S, Chun YK, Kang SS, Hur MH (2017) The Usefulness of Intraoperative Circumferential Frozen-Section Analysis of Lumpectomy Margins in Breast-Conserving Surgery. *J Breast Cancer* 20:176–182 [PubMed: 28690654]
159. Pleijhuis RG, Graafland M, de Vries J, et al. (2009) Obtaining Adequate Surgical Margins in Breast-Conserving Therapy for Patients with Early-Stage Breast Cancer: Current Modalities and Future Directions. *Ann Surg Oncol* 16:2717–2730 [PubMed: 19609829]
160. Petropoulou T, Kapoula A, Mastoraki A, et al. (2017) Imprint cytology versus frozen section analysis for intraoperative assessment of sentinel lymph node in breast cancer. *Breast cancer (Dove Med Press)* 9:325–330 [PubMed: 28503075]
161. Barth CW, Schaefer JM, Rossi VM, et al. (2017) Optimizing fresh specimen staining for rapid identification of tumor biomarkers during surgery. *Theranostics* 7:4722–4734 [PubMed: 29187899]
162. Hutteman M, Choi HS, Mieog JSD, et al. (2011) Clinical translation of ex vivo sentinel lymph node mapping for colorectal cancer using invisible near-infrared fluorescence light. *Ann Surg Oncol* 18:1006–1014 [PubMed: 21080086]
163. Cutter JL, Cohen NT, Wang J, et al. (2012) Topical application of activity-based probes for visualization of brain tumor tissue. *PLoS One* 7:e33060
164. Tipirneni KE, Warram JM, Moore LS, et al. (2017) Oncologic Procedures Amenable to Fluorescence-guided Surgery. *Ann Surg* 266:36–47 [PubMed: 28045715]
165. Tummers WS, Warram JM, Tipirneni KE, et al. (2017) Regulatory Aspects of Optical Methods and Exogenous Targets for Cancer Detection. *Cancer Res* 77:2197 LP-2206 [PubMed: 28428283]
166. Mondal SB, Gao S, Zhu N, et al. (2015) Binocular Goggle Augmented Imaging and Navigation System provides real-time fluorescence image guidance for tumor resection and sentinel lymph node mapping. *Sci Rep* 5:12117 [PubMed: 26179014]
167. Mondal SB, Gao S, Zhu N, et al. (2017) Optical See-Through Cancer Vision Goggles Enable Direct Patient Visualization and Real-Time Fluorescence-Guided Oncologic Surgery. *Ann Surg Oncol* 24:1897–1903 [PubMed: 28213790]
168. Boogerd LSF, Hoogstins CES, Schaap DP, et al. (2018) Safety and effectiveness of SGM-101, a fluorescent antibody targeting carcinoembryonic antigen, for intraoperative detection of colorectal cancer: a dose-escalation pilot study. *Lancet Gastroenterol Hepatol* 3:181–191 [PubMed: 29361435]
169. Payne WM, Hill TK, Svechkarev D, et al. (2017) Multimodal Imaging Nanoparticles Derived from Hyaluronic Acid for Integrated Preoperative and Intraoperative Cancer Imaging. *Contrast Media Mol Imaging* 2017:1–14
170. Gao N, Bozeman EN, Qian W, et al. (2017) Tumor Penetrating Theranostic Nanoparticles for Enhancement of Targeted and Image-guided Drug Delivery into Peritoneal Tumors following Intraperitoneal Delivery. *Theranostics* 7:1689–1704 [PubMed: 28529645]
171. Biffi S, Petrizza L, Garrovo C, et al. (2016) Multimodal near-infrared-emitting PluS Silica nanoparticles with fluorescent, photoacoustic, and photothermal capabilities. *Int J Nanomedicine* 11:4865–4874 [PubMed: 27703352]

172. Lu Z, Pham TT, Rajkumar V, et al. (2018) A Dual Reporter Iodinated Labeling Reagent for Cancer Positron Emission Tomography Imaging and Fluorescence-Guided Surgery. *J Med Chem* 61:1636–1645 [PubMed: 29388770]
173. Nagaya T, Nakamura Y, Sato K, et al. (2017) Near infrared photoimmunotherapy with avelumab, an anti-programmed death-ligand 1 (PD-L1) antibody. *Oncotarget* 8:8807–8817 [PubMed: 27716622]
174. Maruoka Y, Nagaya T, Nakamura Y, et al. (2017) Evaluation of Early Therapeutic Effects after Near-Infrared Photoimmunotherapy (NIR-PIT) Using Luciferase–Luciferin Photon-Counting and Fluorescence Imaging. *Mol Pharm* 14:4628–4635 [PubMed: 29135265]
175. Sun Q, You Q, Wang J, et al. (2018) Theranostic Nanoplatfrom: Triple-Modal Imaging-Guided Synergistic Cancer Therapy Based on Liposome-Conjugated Mesoporous Silica Nanoparticles. *ACS Appl Mater Interfaces* 10:1963–1975 [PubMed: 29276824]
176. Li X, Schumann C, Albarqi HA, et al. (2018) A Tumor-Activatable Theranostic Nanomedicine Platform for NIR Fluorescence-Guided Surgery and Combinatorial Phototherapy. *Theranostics* 8:767–784 [PubMed: 29344305]
177. Sun Y, Ding M, Zeng X, et al. (2017) Novel bright-emission small-molecule NIR-II fluorophores for in vivo tumor imaging and image-guided surgery. *Chem Sci* 8:3489–3493 [PubMed: 28507722]
178. Cheng K, Chen H, Jenkins CH, et al. (2017) Synthesis, Characterization, and Biomedical Applications of a Targeted Dual-Modal Near-Infrared-II Fluorescence and Photoacoustic Imaging Nanoprobe. *ACS Nano* 11:12276–12291 [PubMed: 29202225]
179. Miao W, Kim H, Gujrati V, et al. (2016) Photo-decomposable Organic Nanoparticles for Combined Tumor Optical Imaging and Multiple Phototherapies. *Theranostics* 6:2367–2379 [PubMed: 27877241]
180. Liu L, Ruan Z, Yuan P, et al. (2018) Oxygen Self-Sufficient Amphiphilic Polypeptide Nanoparticles Encapsulating BODIPY for Potential Near Infrared Imaging-guided Photodynamic Therapy at Low Energy. *Nanotheranostics* 2:59–69 [PubMed: 29291163]

## Fluorescence Image Guided Surgery Instrumentation



## Potential Uses of FIGS in Surgical Oncology

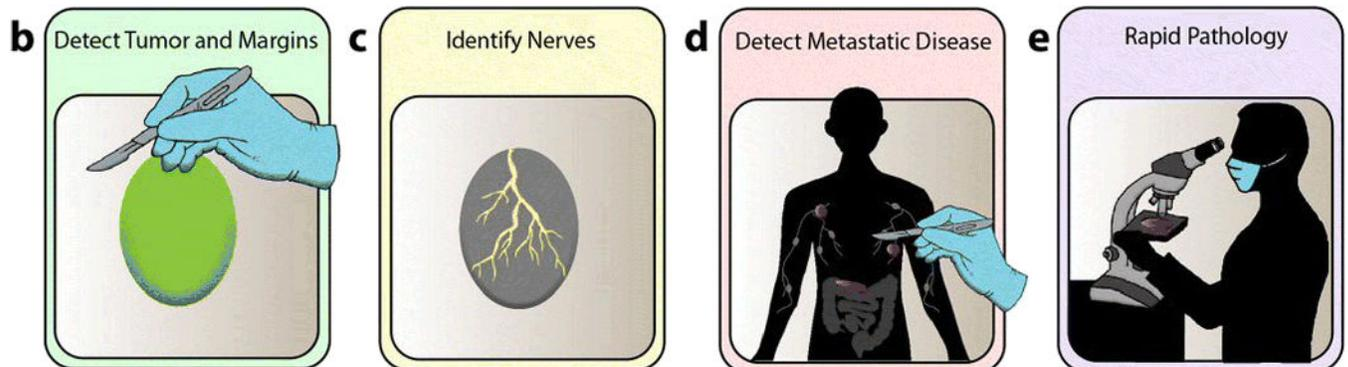


**Figure 1.**

FIGS instrumentation and potential uses: **a** FIGS instrumentation consists of three critical components: an excitation source, a collection source and a display. The excitation source is responsible for exciting the fluorophore, the collection source picks up the fluorophore wavelength and discards other light, and the display provides intraoperative real-time feedback of the surgical field. Contrast agents for FIGS can be used in several formulations, including free dyes, dyes entrapped in nanoparticles, and dyes conjugated to targeting moieties. FIGS has many potential uses in the field of surgical oncology. **b** Surgeons are able to detect tumors and tumor margins with FIGS, which can result in a reduction in recurrence. **c** Additionally, FIGS can be used to identify critical nerves during surgery, to avoid injurious resection. **d** FIGS has shown efficacy in detecting metastasis in addition to the primary tumor, especially lymph nodes. **e** Pathologists can use FIGS for rapid ex vivo analysis of tissue samples, to confirm negative margins.

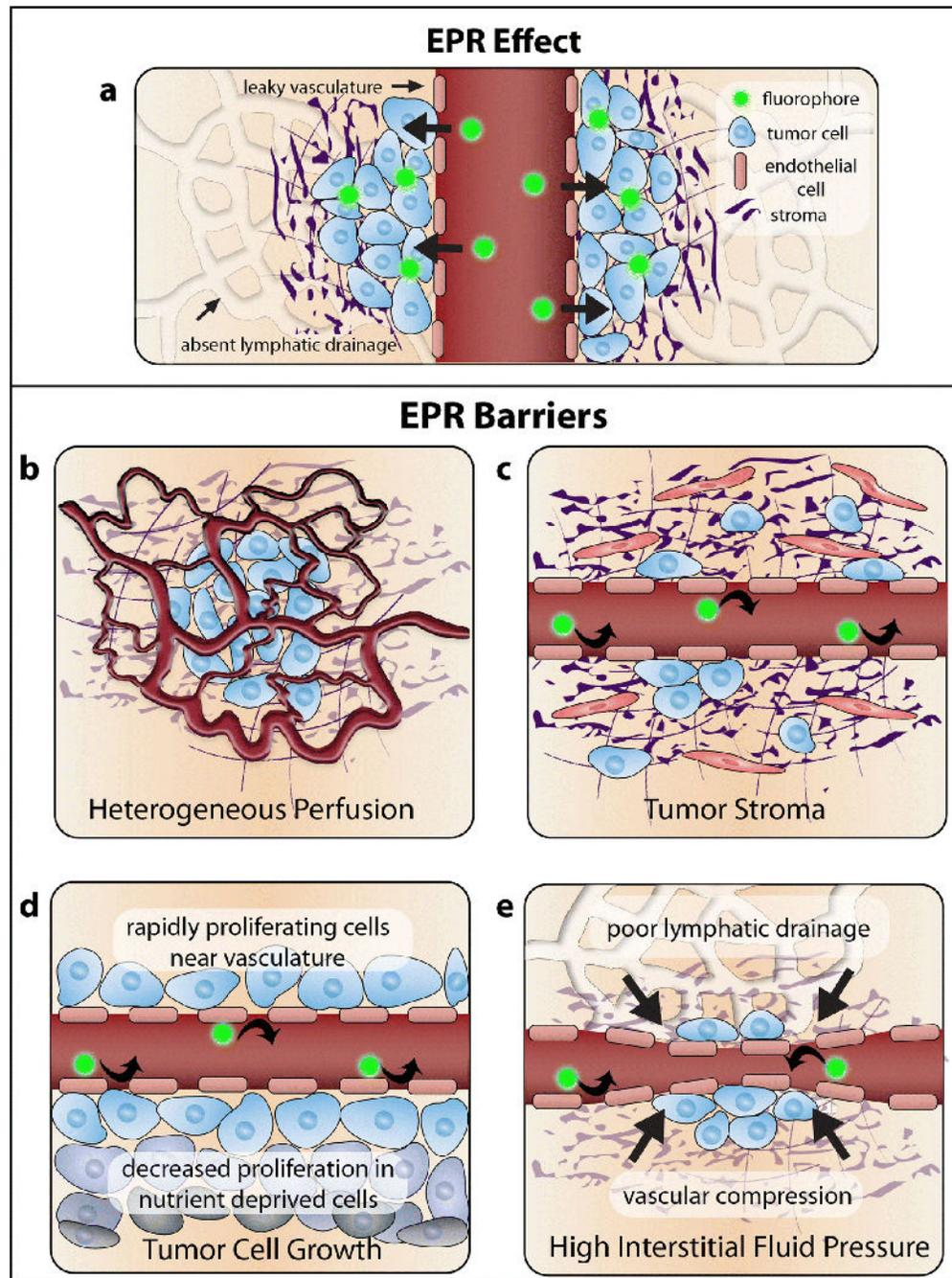


**Figure 2.**

Passive targeting mechanisms and barriers: **a** The strategy of passive targeting for FIGS is based on the enhanced permeability and retention effect in tumors. Contrast agents enter the tumor through the leaky vasculature, and stay in the tumor because of poor drainage. However, there are many barriers to the efficacy of this targeting strategy. **b** Heterogeneous perfusion from abnormal vasculature can result in inadequate perfusion in some areas of the tumor. **c** The presence of a dense tumor stroma can prevent penetration of contrast agents. **d** High gradients of tumor cell growth near to the vasculature can increase pressure and

prevent contrast agents from leaking into the tumor. **e** High interstitial fluid pressure from inadequate lymphatic drainage can also prevent contrast agent deposition.

Author Manuscript

Author Manuscript

Author Manuscript

Author Manuscript

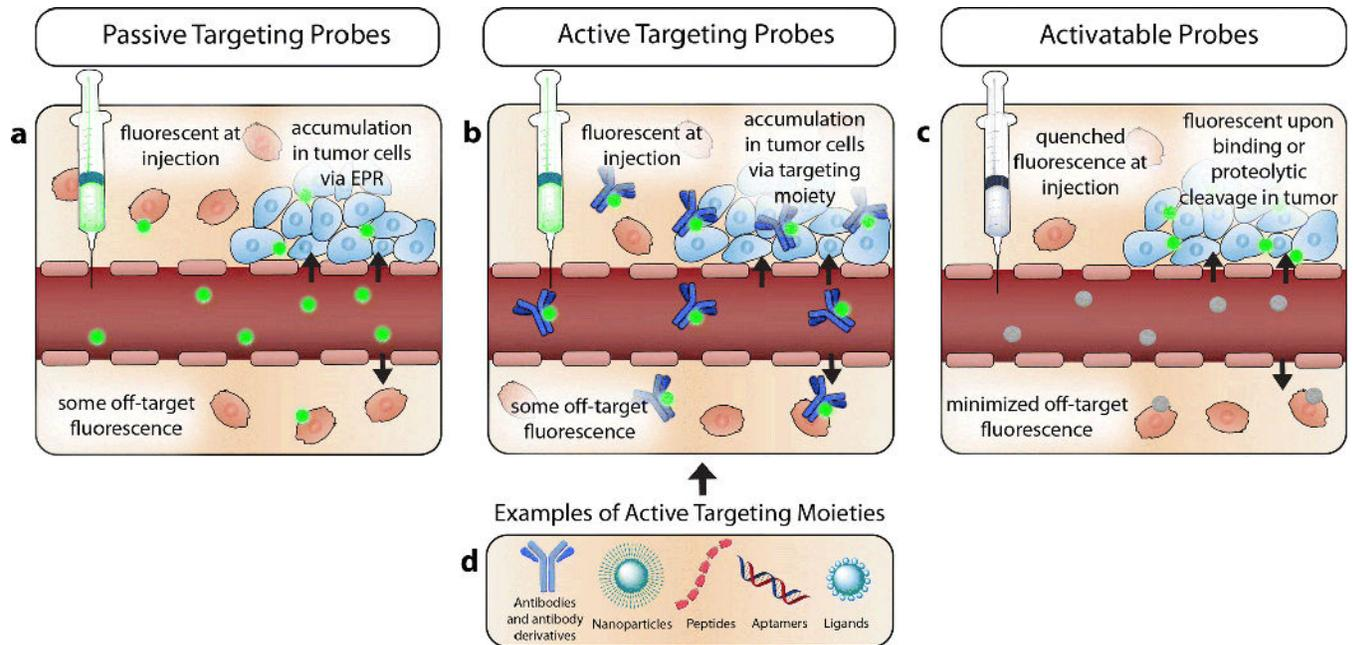


**Figure 3.**

Tumor targeting Strategies: **a** Passive targeting relies on the selective accumulation of contrast agents in the tumor tissue, via leaky vasculature and absent lymph drainage. The contrast agents used in this targeting strategy are fluorescent at injection, and can result in non-specific binding when the contrast agent is deposited outside the confines of the tumor. **b** Active targeting probes rely on a targeting moiety conjugated to a contrast agent to specify fluorescence. **c** Activatable probes exhibit quenched fluorescence when they are injected, or topically applied. Binding to specific antigens, or cleavage by a tumor protease results in the activation of these probes. Therefore, only cells that are targeted fluoresce. **d** There are many moieties available to use for active targeting, including but not limited to; antibodies, antibody derivatives, nanoparticle scaffolds, peptides, ligands, and aptamers.

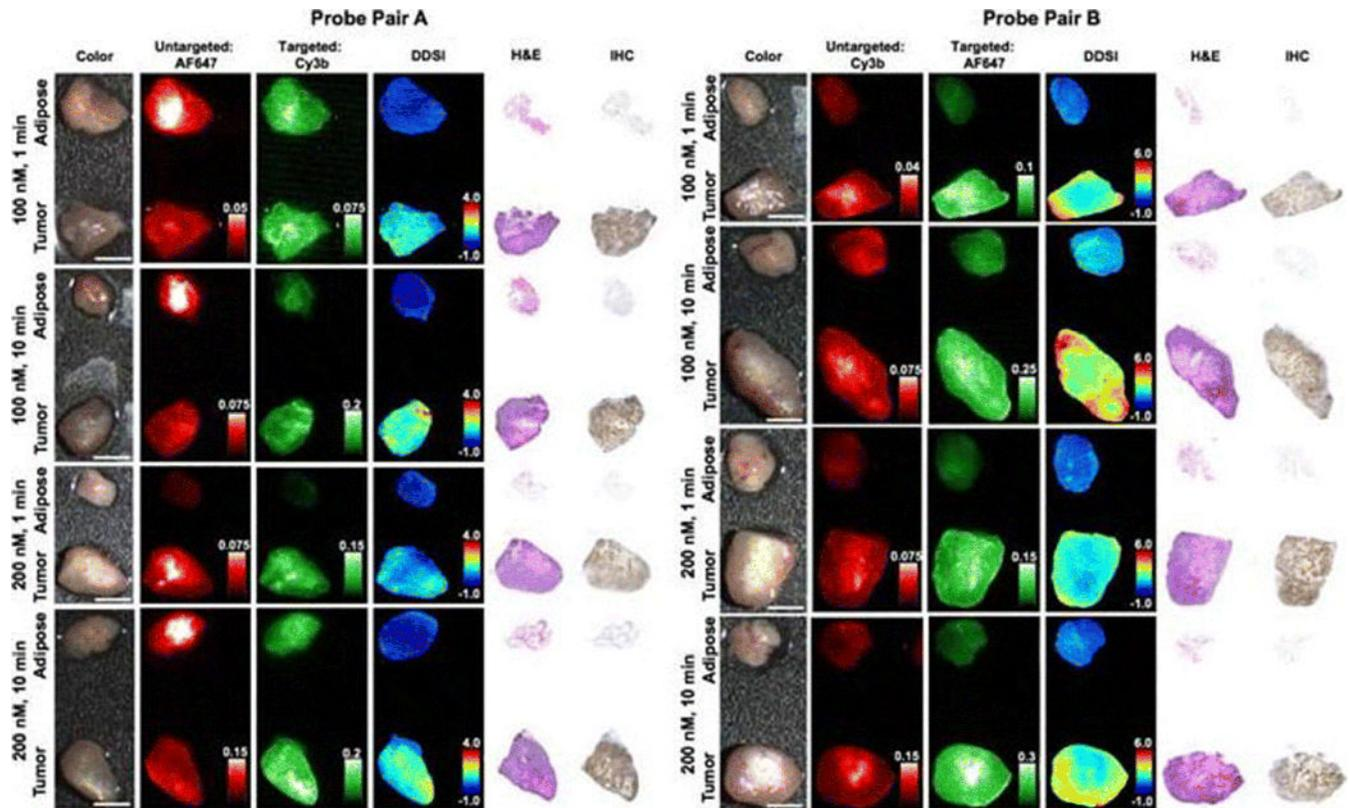


**Figure 4.**

Dual probe *ex vivo* specimen imaging: Representative color, fluorescence, DDSI (dual probe difference specimen imaging), H&E, and HER2 targeted IHC images of tumor and adipose tissue pairs following staining using a range of dual-stain soak concentrations and incubation times for **a** probe pair A (Herceptin-Cy3b, DkRb-AF647) and **b** probe pair B (Herceptin-AF647, DkRb-Cy3b). All images are representative of data collected for  $n=6$  tumor and adipose tissue pairs per staining condition. All untargeted and targeted channel images are background corrected, normalized by their exposure time and calibration drop intensity. DDSI images are displayed with equivalent color scales across staining conditions. H&E and IHC images were acquired from serial sections of the same tissue face imaged in the whole specimen DDSI images. H&E: hematoxylin and eosin; IHC: immunohistochemistry. Scale bars = 5 mm. (Adapted from Barth CW, Schaefer JM, Rossi VM, Davis SC, Gibbs SL. *Optimizing fresh specimen staining for rapid identification of tumor biomarkers during surgery*. *Theranostics* 2017; 7(19):4722–4734. © Ivyspring International Publisher, 2017).

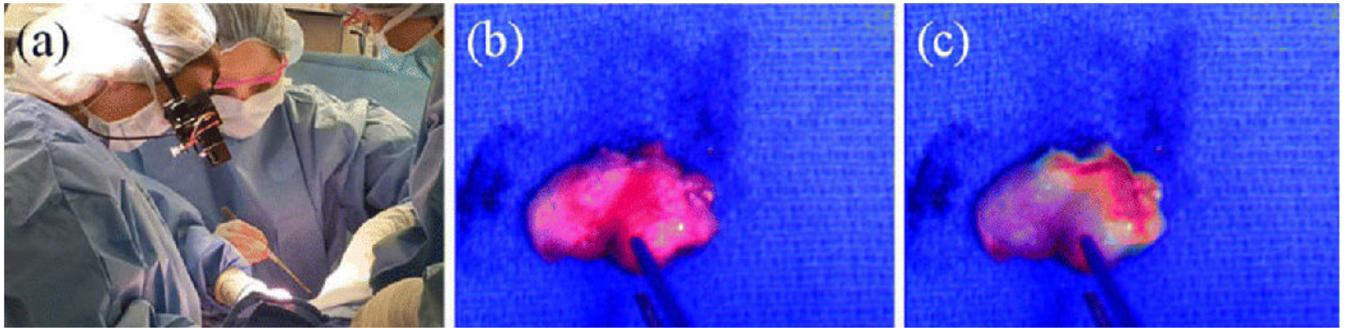


**Figure 5.**

Goggles used for FIGS and cancer detection: Fluorescence-guided SLN biopsy. **a** The surgeon wearing the goggles during SLN visualization in a breast cancer patient. **b** The color image of the excised SLN. **c** The superimposed color-fluorescence image of the excised SLN as seen by the surgeon. (Adapted with permission from Mondal SB, Gao S, Zhu N, et al (2017) *Optical See-Through Cancer Vision Goggles Enable Direct Patient Visualization and Real-Time Fluorescence-Guided Oncologic Surgery. Ann Surg Oncol 24:1897–1903*).

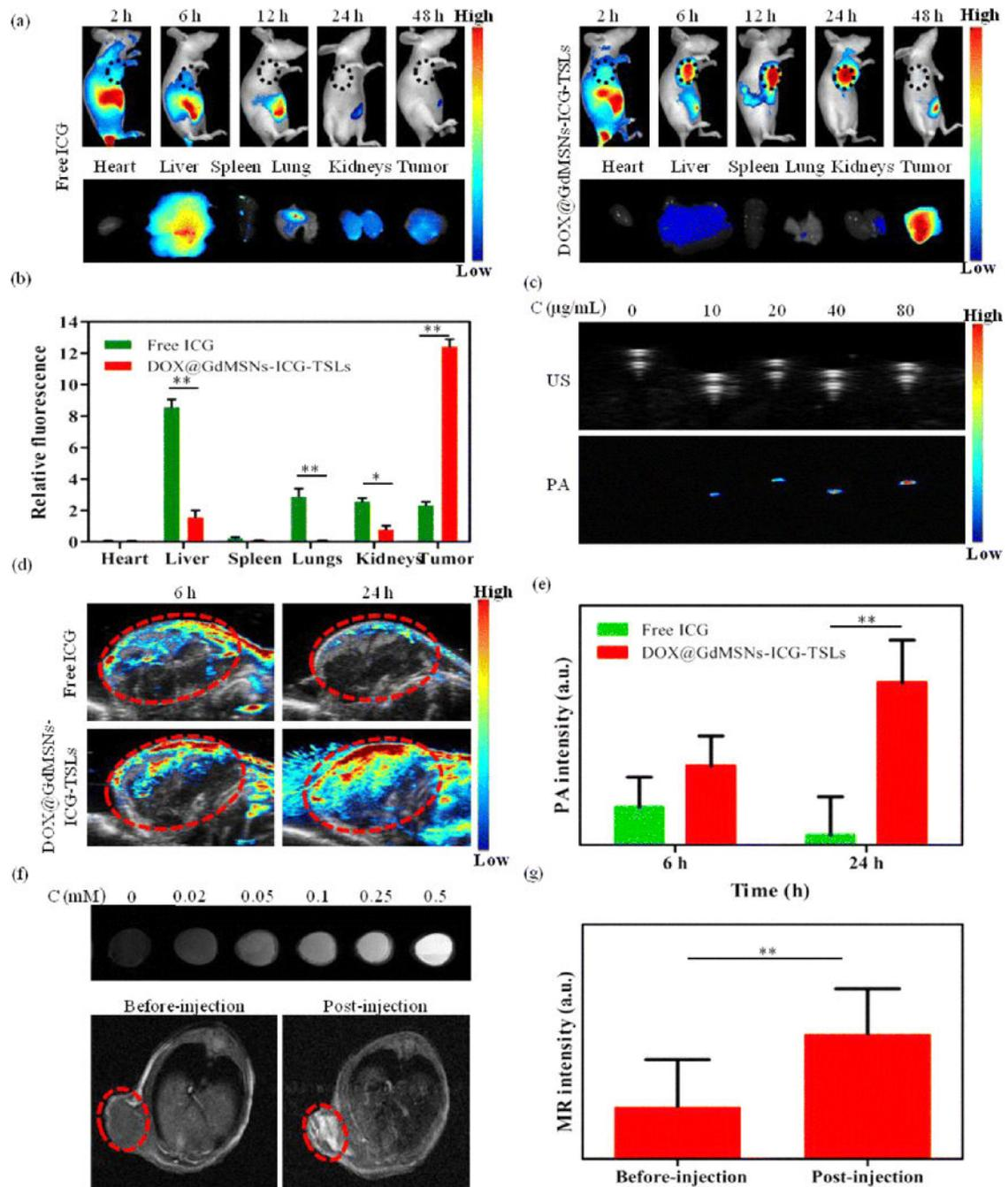


**Figure 6.** Multimodal applications of FIGS: **a** *In vivo* NIR fluorescence images after intravenous injection of free ICG and DOX@GdMSNs-ICG-TSLs in tumor-bearing mice at 2, 6, 12, 24, and 48 h, and the corresponding fluorescence images of different tissues after treated with free ICG and DOX@GdMSNs-ICG-TSLs at 24 h. **b** Relative fluorescence intensity of ICG in major organs induced by 808 nm laser (1.5 W/cm<sup>2</sup>) irradiation at 24 h after i.v. administration. **c** US and PA images of DOX@GdMSNs-ICG-TSLs at various concentrations of ICG. **d** PA images of tumor-bearing mice after 6 and 24 h intravenous

injection via tail of free ICG and DOX@GdMSNs-ICG-TSLs, respectively. **e** PA intensity of tumor sites after treatment with free ICG and DOX@GdMSNs-ICG-TSLs at 6 and 24 h. **f** T1-weighted MR images (7 T, spin-echo sequence; repetition time, TR = 500 ms; echo time, TE = 14.92 ms) of DOX@GdMSNs-ICG-TSLs nanoparticles at various Gd concentrations. And T1-weighted MR images of tumor-bearing mice before and after injected with DOX@GdMSNs-ICG-TSLs for 24 h. **g** Relative MR intensity before and after injecting DOX@GdMSNs-ICG-TSLs. Data are presented as means  $\pm$  SD (n = 5); \*P < 0.05, \*\*P < 0.01. (Adapted with permission from Sun Q, You Q, Wang J, et al (2018) *Theranostic Nanoplatform: Triple-Modal Imaging-Guided Synergistic Cancer Therapy Based on Liposome-Conjugated Mesoporous Silica Nanoparticles*. ACS Appl Mater Interfaces © 2018 American Chemical Society).

**Table 1.**

Summary of Select Contrast Agents for use in FIGS

Fluorophore	Excitation/Emission (nm)	Target	Applications in FIGS	Approval Phase	References
<b>5-ALA</b>	405/635	Non-specific	Glioma detection	FDA approved	[41–46]
<b>Methylene Blue</b>	665/686	Non-specific	Vital structure detection, SLN, tumor detection	FDA approved	[28–40]
<b>ICG</b>	80/822	Non-specific	SLN, reconstruction, tumor detection	FDA approved	[23,47–54]
<b>IRDye800CW</b>	774/789	Non-specific, conjugatable	Tumor detection and imaging	Clinical Trials	[23,55–57]
<b>Dy800</b>	777/791	Non-specific, conjugatable	Tumor detection and imaging	Pre-clinical	[62–64]
<b>Other Cyanine dyes</b>	Cy 5 – 658/666 Cy 5.5 – 679/696 Cy 7 – 747/774 Cy 7.5 – 788/808	Non-specific, conjugatable	Tumor detection and imaging	Pre-clinical	[23,59,65]
<b>Quantum Dots</b>	700–1500	Non-specific, conjugatable	Tumor detection and imaging	Pre-clinical	[23,58]

**Table 2.**

## Representative Clinical Trials Utilizing FIGS

	Objective	Trial Identification	Cancer Type
Indocyanine Green (ICG)	Lymph Node Detection	NCT03297957	Head and Neck
		NCT02840617	Prostate
		NCT02068820	Endometrial
		NCT01562106	Endometrial
		NCT02209532	Endometrial, Uterine, Cervical
		NCT02131558	Endometrial
		NCT03321448	Cervical
		NCT01818739	Endometrial
		NCT02478138	Head, Neck, Oral
		NCT02168452	Breast
		NCT01673022	Endometrial, Cervical
		NCT02316795	Breast, Melanoma
		NCT02119858	Prostate
		NCT02869152	Rectal
		NCT02850783	Colon
		NCT02423148	Lung
		NCT02817334	Breast
		NCT03320772	Cervical
		NCT02419807	Breast
	NCT01926743	Gastric	
	Tumor Detection	NCT02611245	Lung, Esophageal
		NCT02027831	Head and Neck
		NCT01281488	Renal
NCT01738217		Liver	
NCT02473159		Breast	
NCT02479997		Breast	
NCT02172989		Breast	
NCT02032485	Colon		
Surgical Reconstruction	NCT02629029	Head and Neck Neoplasms	
5-ALA	Tumor Detection	NCT01837225 NCT03058705	Breast Bladder
		NCT00285701	Colon (dose finding)
		NCT00752323	Brain and CNS (dosing)
	Spatial Correlation and Modality Agreement	NCT00870779	Brain
IRDye800CW	Localization, Safety, Detection	NCT01508572	Breast
	Signal Detection	NCT03282461	Head and Neck
		NCT01972373	Rectal

	Objective	Trial Identification	Cancer Type
		<a href="#">NCT03154411</a>	Soft tissue Sarcoma
		<a href="#">NCT03134846</a>	Head and Neck
		<a href="#">NCT02129933</a>	Esophageal
		<a href="#">NCT02583568</a>	Breast
	Dose/Safety and Detection	<a href="#">NCT03384238</a>	Pancreatic
		<a href="#">NCT02901925</a>	Glioma
		<a href="#">NCT02497599</a>	Renal
<b>Other</b>	OTL38 Safety and detection	<a href="#">NCT02872701</a>	Lung
		<a href="#">NCT03180307</a>	Ovarian
	SGM-101 Safety and detection	<a href="#">NCT02973672</a>	Colon, rectum, pancreas
	LUM015 Safety and Detection	<a href="#">NCT02438358</a>	Breast
		<a href="#">NCT03321929</a>	Breast
		<a href="#">NCT02584244</a>	Gastrointestinal
		<a href="#">NCT03441464</a>	Prostate

Search terms: "fluorescence imaging"

Exclusion criteria: withdrawn, terminated, suspended clinical trials